RESEARCH ARTICLE

The intricate cellular ecosystem of human peripheral veins as revealed by single-cell transcriptomic analysis

Miguel G. Rojas[1], **Zachary M. Zigmond**[2], **Simone Pereira-Simon**[1], **Nieves Santos Falcon**[1], **Maya Suresh Kumar**[1], **Filipe F. Stoyell-Conti**[1], **Christina Kosanovic**[3], **Anthony J. Griswold**[3], **Alghidak Salama**[1], **Xiaofeng Yang**[4], **Marwan Tabbara**[1], **Roberto I. Vazquez-Padron**[1,2]*, **Laisel Martinez**[1]*

1 DeWitt Daughtry Family Department of Surgery, Leonard M. Miller School of Medicine, University of Miami, Miami, Florida, United States of America, **2** Bruce W. Carter Veterans Affairs Medical Center, Miami, Florida, United States of America, **3** John P. Hussman Institute for Human Genomics, Leonard M. Miller School of Medicine, University of Miami, Miami, Florida, United States of America, **4** Department of Cardiovascular Sciences, Lewis Katz School of Medicine at Temple University, Philadelphia, Pennsylvania, United States of America

* lmartinez6@med.miami.edu (LM); rvazquez@med.miami.edu (RIVP)

🔓 OPEN ACCESS

Abstract

The venous system has been historically understudied despite its critical roles in blood distribution, heart function, and systemic immunity. This study dissects the microanatomy of upper arm veins at the single cell level, and how it relates to wall structure, remodeling processes, and inflammatory responses to injury. We applied single-cell RNA sequencing to 4 non-diseased human veins (3 basilic, 1 cephalic) obtained from organ donors, followed by bioinformatic and histological analyses. Unsupervised clustering of 20,006 cells revealed a complex ecosystem of endothelial cell (EC) types, smooth muscle cell (SMCs) and pericytes, various types of fibroblasts, and immune cell populations. The venous endothelium showed significant upregulation of cell adhesion genes, with arteriovenous zonation EC phenotypes highlighting the heterogeneity of vasa vasorum (VV) microvessels. Venous SMCs had atypical contractile phenotypes and showed widespread localization in the intima and media. $MYH11^+DES^{lo}$ SMCs were transcriptionally associated with negative regulation of contraction and pro-inflammatory gene expression. $MYH11^+DES^{hi}$ SMCs showed significant upregulation of extracellular matrix genes and pro-migratory mediators. Venous fibroblasts ranging from secretory to myofibroblastic phenotypes were 4X more abundant than SMCs and widely distributed throughout the wall. Fibroblast-derived angiopoietin-like factors were identified as versatile signaling hubs to regulate angiogenesis and SMC proliferation. An abundant monocyte/macrophage population was detected and confirmed by histology, including pro-inflammatory and homeostatic phenotypes, with cell counts positively correlated with age. Ligand-receptor interactome networks identified the venous endothelium in the main lumen and the VV as a niche for monocyte recruitment and infiltration. This study underscores the transcriptional uniqueness of venous cells and their relevance for vascular inflammation and remodeling processes. Findings from this study may be relevant for molecular investigations of upper arm veins used for vascular access

creation, where single-cell analyses of cell composition and phenotypes are currently
lacking.

Introduction

The systemic venous system is an often-underappreciated component of the cardiovascular
system, with critical roles in blood distribution, heart function, and even systemic immunity.
Research of vein biology has historically relied on extrapolations from arterial biology, despite
differences in structure, functions, hemodynamics, and propensity to diseases. In the last two
decades, transcriptomic studies have provided in-depth characterizations of molecular pro-
cesses in healthy and diseased human arteries [1–5], but little attention has been paid to
human veins [6–8]. This paucity of data limits our understanding of venous pathologies and of
cells populating half of the circulatory system.

Recently, single-cell RNA sequencing has revealed an unappreciated level of cellular hetero-
geneity, identified unknown cell types, and elucidated cellular differentiation and interaction
pathways associated with atherosclerosis and aortic aneurysms [2, 4, 5, 9–11]. However, the
perturbations in cellular ecology underlying venous diseases such as thrombophlebitis, deep
vein thrombosis, and chronic vein insufficiency remain unknown. Peripheral veins, in particu-
lar, are commonly affected by stenotic remodeling after their use for vein grafts or creation of
arteriovenous fistulas (AVF) for hemodialysis [12–14]. The frequency of these complications,
prevalence of chronic venous diseases, and their significant contribution to patient mortality
and morbidity stress the need for high-throughput discovery methods to dissect cellular
dynamics within the healthy and diseased venous wall.

Histological inspection of human saphenous and upper extremity veins shows structural
wall irregularities regardless of age or the presence of common comorbidities [15–20]. Fre-
quent characteristics include medial atrophy, disorganized smooth muscle cells (SMCs), inti-
mal hyperplasia (IH), and abundant interstitial extracellular matrix (ECM) suggesting a
natural tendency to wall fibrosis [14, 15, 17–22]. The absence or thinning of the internal elastic
lamina (IEL) and the abundance of fragmented elastic fibers scattered across the wall may have
important implications for cell migration and inflammation [16, 22, 23]. The interstitial space
between SMC bundles seems to be populated by cells of unknown lineages [16]. Endothelial
defects and intramural vascularization that ranges from protective to pathogenic have also
been described [18, 20, 24–27]. Despite all available knowledge of venous histology, how these
characteristics relate to normal physiology or disease is unclear. Thus, as in studies of arteries,
single-cell analyses hold great promise to understand the relationship between those unique
structural characteristic and venous function.

In this study, we generate a detailed single-cell transcriptomic atlas of upper extremity veins
with histological validations. We reveal a complex ecosystem of ECs with various arteriove-
nous zonation phenotypes, and an interactive network of discrete SMC populations, different
types of fibroblasts, and abundant immune cells in the venous wall. Our analyses support a
role for ECs in the main lumen and vasa vasorum (VV) venules, SMCs, and pericytes in pro-
moting immune cell recruitment and infiltration. We also support a protagonist role of fibro-
blasts and atypical SMCs in angiogenesis and wall remodeling. Overall, this work constitutes
an essential foundation for the study of veins commonly used for vascular access creation and
the peripheral venous system in general.

Results

Single-cell RNA sequencing of upper arm veins

A representative cross-section of a medium-size peripheral vein is characterized by 1) low to moderate IH, 2) a thin or fragmented IEL, 3) circular or diagonally oriented cells between the IEL and longitudinal smooth muscle fibers, 4) medial SMC bundles intercalated in abundant ECM, 5) fragmented elastic fibers in the adventitia, and 6) numerous VV in the outer layers of the vessel (Fig 1A, S1 Fig). To explore this microanatomy in further detail, cell suspensions were obtained from three basilic and one cephalic vein collected from the upper arms of organ donors and analyzed using single-cell RNA sequencing (S2 Fig). The group of donors was highly variable in terms of age (26–70 years), sex (50:50), and ethnic distribution (2 whites, 1 Hispanic, 1 black) (S1 Table). Causes of death included head trauma (26F and 64M), cardio-vascular (38F), and cerebrovascular events (70M). One donor had history of hypertension (38F) and none had diabetes. We did not observe significant differences in morphometry between upper arm basilic and cephalic veins (S1 Fig), in agreement with published data [15].

Fig 1B presents a coarse clustering map of 20,006 cells, with proportions of cell populations separated by sample identity (Fig 1C, S2C Fig). Fibroblasts (14–47%) and monocyte/macro-phages (18–44%) had the highest cell proportions in individual samples, followed by ECs (8–10%), SMCs (7–22%), and T cells (1–26%; Fig 1C). The top Seurat markers for SMC identification were contractile genes (*ACTA2*, *TAGLN*, *MYH11*, *CNN1*), extracellular matrix genes and complement factors in fibroblasts (*DCN*, *LUM*, *COL1A1*, *CFD*), cell adhesion molecules and
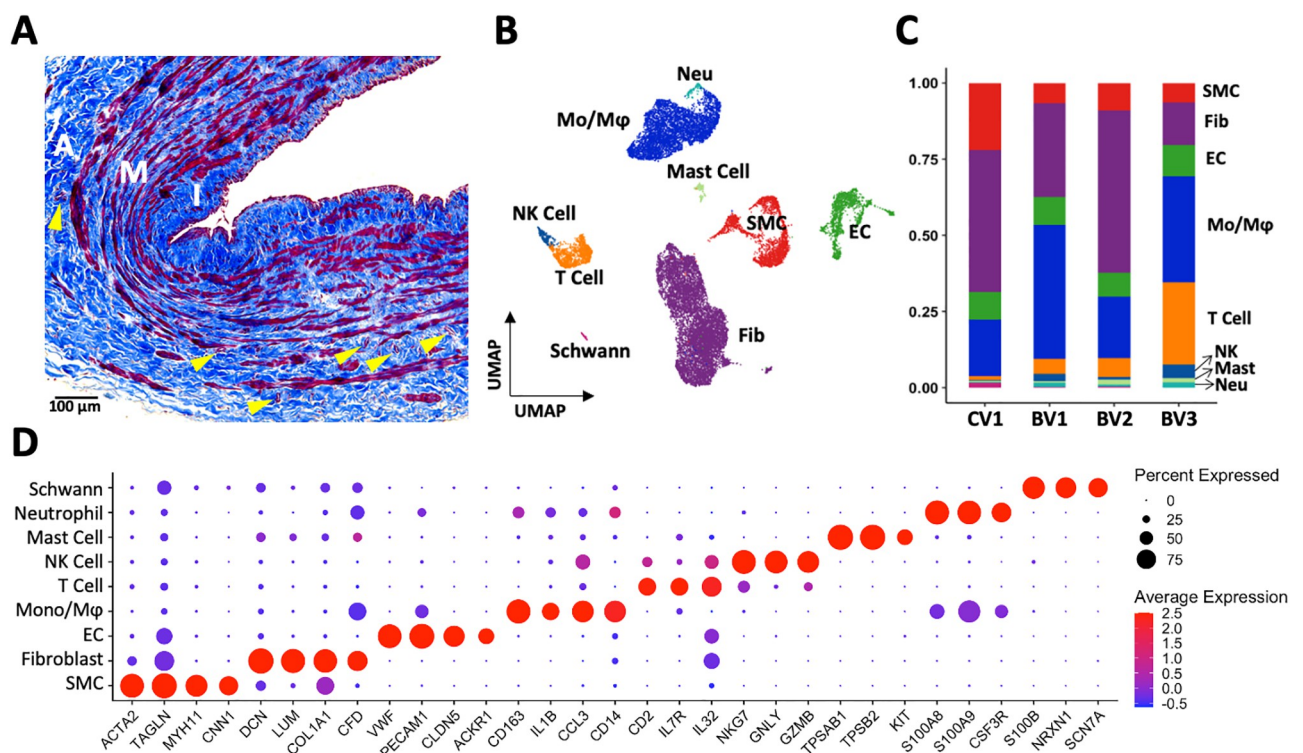
Fig 1. Wall structure and cell composition of upper arm veins. A) Representative Masson's trichrome stained cross-section of a basilic vein, indicating the intimal (I), medial (M), and adventitial (A) layers. Cells are stained in red while extracellular matrix appears in blue. Vasa vasorum are indicated by yellow arrowheads. **B-C)** Uniform manifold approximation and projection (UMAP) plot of 20,006 cells isolated from 4 veins (1 cephalic [CV1], 3 basilic [BV1-3]) and proportion of cell types per vein sample. **D)** Markers used for cell cluster identification.

https://doi.org/10.1371/journal.pone.0296264.g001

tight junction proteins in ECs (*VWF*, *PECAM1*, *CLDN5*, *ACKR1*), and various cell surface receptors and secreted factors for immune cell populations (monocytes/macrophages, *CD163*, *IL1B*, *CCL3*, *CD14*; neutrophils, *S100A8/9*, *CSF3R*; T cells, *CD2*, *IL7R*, *IL32*; NK cells, *NKG7*, *GNLY*, *GZMB*; mast cells, *TPSAB1*, *TPSB2*, *KIT*) (Fig 1D). Lastly, we found a small Schwann cell population defined by *S100B*, *NRXN1*, and *SCN7A*, likely originating from periadventitial neurovascular tissue (Fig 1D). We then proceeded to characterize these main populations in detail, focusing on subpopulation gene expression profiles, localization, and cell-to-cell communication networks.

A pro-inflammatory endothelium in upper arm veins

Endothelial cells are one of the most heterogenous populations in peripheral veins due to the presence of valves and the abundant VV irrigating the venous wall. The proportion of ECs ranged from 7.8 to 10.1% across the 4 veins analyzed (Fig 1C), for a total of 1,695 cells out of 20,006 in the focused uniform manifold approximation and projection (UMAP) plot (Fig 2A). These subdivided into five groups corresponding to arteriovenous zonation phenotypes annotated elsewhere [6, 28–30]: EC1 [arteriolar-like], 215 cells; EC2 [capillary-like], 400; EC3 [venous-like], 712; EC4 [valvular-like], 257; and EC5 [lymphatic-like], 111 (Fig 2). Canonical
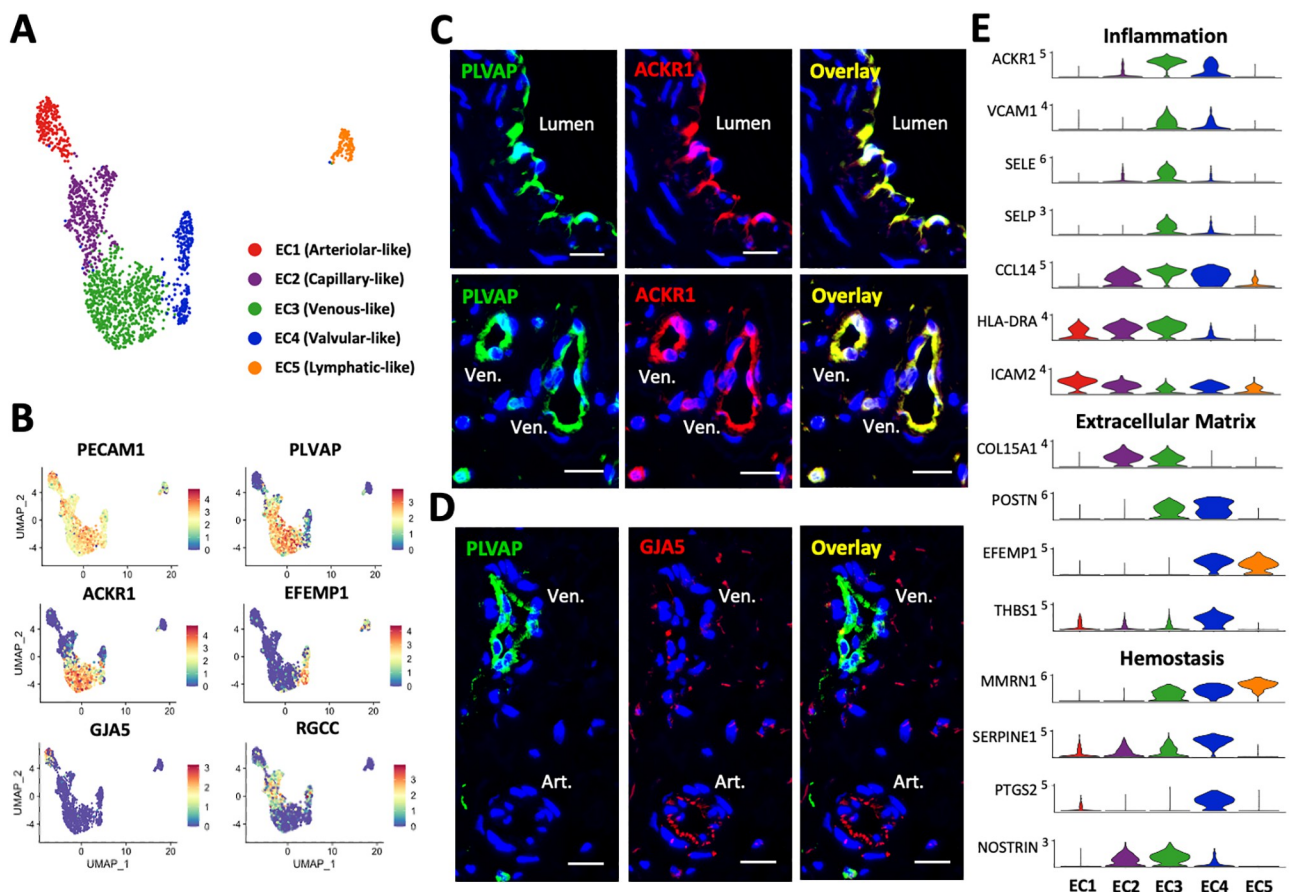
Fig 2. Endothelial cells (EC) in upper arm veins. A) Focused UMAP of 1,695 ECs isolated from upper arm veins. **B)** Feature plots indicating normalized expression levels of markers characteristic of the 5 EC populations. **C-D)** Identification of venous (PLVAP⁺ACKR1⁺) and arteriolar (PLVAP⁻GJA5⁺) ECs in the main lumen of veins and vasa vasorum by immunofluorescence. Ven. = venule; Art. = arteriole. Scale bars represent 20 μm in all panels. **E)** Violin plot representation of expression differences among the 5 EC populations.

markers in common among all EC subsets were *CDH5*, *CLDN5*, *ERG*, *PECAM1*, and *VWF* (Fig 1D), while markers characterizing each population are presented in S3A Fig and Table 1.

There is a continuum of transcriptional regulation across the five EC populations as demonstrated using pseudotime trajectory analysis (S3B Fig). From arteriolar-like (EC1) to lymphatic-like ECs (EC5), there is a decreasing expression gradient in arterial differentiation factors such as *NOTCH4*, *SOX17*, and *HEY1* (Moran's I = 0.34 to 0.43, padj<0.001) and the opposite trend in the venous differentiation factor *NR2F2* (Moran's I = 0.43). Levels of *FOXC2*, which is linked to primary venous valve failure and lymphedema when mutated [31], also increase from valvular to lymphatic ECs (Moran's I = 0.49; S3B Fig). Factors upregulated in venous ECs with respect to the other populations include *ZNF385D* and *MRTFB* (**S1 File in** S1 Data). Bidirectional signaling between the *EPHB4* receptor in venous ECs and ephrin B2 ligand (*EFNB2*) in arterial ECs is critical for vasculature development in the embryo [32, 33], and thought to be relevant for remodeling of veins after arteriovenous anastomosis [34]. In our dataset, the expression pattern of *EFNB2* does show a decreasing gradient from arteriolar- to venous-like ECs, but *EPHB4* does not discriminate among the different EC subclusters (S3B Fig). This latter observation agrees with IF staining of arteries and veins from adult tissues [35]. As expected, capillary-like ECs co-express high levels of both arterial and venous differentiation factors, such as *NOTCH4* and *NR2F2* (S3B Fig), as well as other genes characteristic of arteriolar (e.g., *ADGRF5*, *CXCL12*, *IGFBP3*) and venous populations (e.g., *COL15A1*, *NOSTRIN*, *PLVAP*) (**S1 File in** S1 Data). This overlap may reflect the size spectrum of microvessels in capillary networks [28, 36], but we lack the resolution for better definition.

The most abundant EC subpopulation in human peripheral veins is the venous-like cluster that lines the main lumen as well as VV venules (Fig 2A–2C, S4 Fig). These are transcriptionally defined by *ACKR1*, *SELE*, *SELP*, *TLL1*, *VCAM1*, and *ZNF385D* (S3A Fig) and are positive for PLVAP and ACKR1 by immunofluorescence (IF) (Fig 2C and 2D, S4A Fig). Localization of ACKR1 in the main lumen of veins demonstrates that this marker is not restricted to postcapillary venules as reported in mice [37]. The transcriptional program of venous ECs highlights unique hemostatic, cell adhesive, and inflammatory properties of the venous endothelium. High expression of plasmalemma vesicle-associated protein (*PLVAP*) and aquaporin 1 (*AQP1*) with respect to other subsets illustrates an environment of increased vascular permeability [38]. In addition, upregulated levels of adhesion molecules *ACKR1*, *ICAM1*, *VCAM1*, *SELE*, and *SELP* showcase these cells as a primed docking site for leukocyte infiltration, as predicted by gene ontology (GO) pathways (Fig 2E, S5A Fig). The vast majority of venous ECs are high expressors of *CCL14* (≥3 normalized copies in a scale of 0–5), a known activator of monocytes along with 188 (26.4%) and 445 out of 712 (62.5%) cells that show upregulation of *IL6* and *IL1R1* (≥1 normalized copy, 0–4 scale for both), respectively, likely indicating inflammatory activation. Upregulation of the nitric oxide synthase trafficker *NOSTRIN* in venous-like and capillary-like cells compared to the rest of ECs (Fig 2E) suggests that eNOS is preferentially located away from the membrane, with important consequences for hemostasis, vasoreactivity, and inflammation. In addition, the abundance of *EPB41L3* and *COL15A1* in venous ECs suggests a low predisposition for endothelial-mesenchymal transformation due to SNAI1 inhibition (S3C Fig) [39, 40].

While smaller in cell count, the arteriolar-like and capillary-like EC subclusters are also important contributors to the VV. Arteriolar ECs cells are characterized by expression of *GJA5*, *HEY1*, *ICAM2*, *NEBL*, *PLLP*, *SEMA3G*, *SYT1*, and *TSPAN2*. These cells stained negative for PLVAP while positive for GJA5 (Fig 2D, S4B Fig). Interestingly, they also showed upregulation of ICAM2 compared to other EC types, and in contrast with ICAM1 and the rest of the adhesion molecules which show higher levels in venous ECs (Fig 2E, **S1 File in** S1 Data). Expression of ICAM2 is thought to be a characteristic of a resting endothelium, where it can

Table 1. Marker genes for cell cluster and subcluster identification and their predicted functions in upper arm veins.

Cluster/Subcluster*	Marker Genes	Classification/Predicted Function
Endothelial cells	VWF, PECAM1, CDH5	Pan-EC markers
EC1–Arteriolar	NOTCH4, SOX17, HEY1	Arterial EC differentiation
	EFNB2, SEMA3G	Angiogenesis
	NEBL, TSPAN2	Cytoskeleton organization
	GJA5	Gap junction
EC2–Capillary	CA4, FMO2, RBP7	pH and redox homeostasis
	CD300LG	Leukocyte binding/rolling
	CD36	Fatty acid uptake
	RGCC	Cell cycle regulation
EC3–Venous	NR2F2	Venous EC differentiation
	PLVAP, AQP1	Permeability
	ACKR1	Chemokine transcytosis
	ICAM1, VCAM1, SELE, SELP	Leukocyte adhesion
EC4–Valvular	FOXC2	Valvular EC differentiation
	CRTAC1, EFEMP1, POSTN, HAPLN3	Extracellular matrix (ECM)
	BMP2, GDF7	ECM synthesis
	SERPINE1, PTGS2	Hemostasis
EC5–Lymphatic	FOXC2, NR2F1, PROX1	Lymphatic EC differentiation
	LYVE1, PDPN, RELN	Leukocyte trafficking
Smooth muscle cells	ACTA2, SRF, MRTFA, MRTFB	Pan-SMC/pericyte markers
SMC1–Desmin^{high}	MYH11, CALD1, TAGLN	SMC contraction
	DES, CNN1, MYLK, ADRA2C	Regulation of contraction
	FN1, COL1A2, COL3A1, VCAN	ECM
	ITGA5, ITGA8	ECM binding
SMC2–Desmin^{low}	MYH11, CALD1, TAGLN	SMC contraction
	PLN, SORBS2, NET1, RERGL, HRH2, ADRA2A	Regulation of contraction
	NDUFA4L2	Low-oxygen sensing
	PGF	Angiogenesis; inflammation
SMC3–Pericyte	CD36, APOE, STEAP4, FABP4	Fatty acid uptake/metabolism
	CYGB	Oxygen diffusion
	EDNRB	Vasoreactivity
	THY1	Stemness; leukocyte infiltration
Fibroblasts	PDGFRA, LUM, C1R, DCN, THY1	Pan-fibroblast markers
Fib1–Activated	COL1A1, COL1A2, COL3A1, BGN, POSTN, FN1	ECM; cell migration
	ACTA2, TAGLN, NREP	Myofibroblastic transition
	NDUFA4L2	Low-oxygen sensing
	F2R	Hemostasis
	ITGA10	ECM binding
Fib2–Maintenance	COL1A1, COL1A2, COL3A1, BGN	ECM
	NDUFA4L2	Low-oxygen sensing
Fib3–Secretory	C1S, C3, CFD	Complement factors
	CD34, CXCL14, SFRP1, SVEP1	Regulation of angiogenesis
	APOD, IGF1, IGFBP5, PLA2G2A, PLPP3, GPX3, MGST1	Lipid metabolism
	SCARA5	Ferritin-iron uptake; adipocytic commitment
Monocyte/ macrophages	CD163, CD14, FCGR3A, MRC1	Pan-mo/mφ markers

(Continued)

Table 1. (Continued)

Cluster/Subcluster*	Marker Genes	Classification/Predicted Function
Mo/Mφ1–IL1B⁺	*IL1B, NLRP3, EREG, CCL20, TNF*	Inflammation
Mo/Mφ2–IL1B⁻	C1QA, C1QB, C1QC, VSIG4	Inflammation resolution
	SELENOP	Redox homeostasis
	FOLR2	Folate uptake

https://doi.org/10.1371/journal.pone.0296264.t001

negatively regulate ICAM1-mediated transendothelial migration of leukocytes [41]. The lower levels of ICAM2 in venous ECs further supports their protagonist role in leukocyte infiltration and higher pro-inflammatory potential. Capillary-like ECs, in turn, are defined by *CA4, CD300LG, CD36, FCN3, FMO2, H19, RBP7, RGCC,* and *TCF15*, and likely correspond to the vast capillary network [24].

Valvular-like ECs have a distinct transcriptional profile from the non-valvular venous population, characterized by high expression of *ANGPTL4, BMP2, CLU, CRTAC1, EFEMP1, HHIP, PTGS2,* and *SERPINE1*. The transcriptional program in this subcluster is directed at ECM production (Fig 2E, S5A Fig), including extracellular proteins *CRTAC1, EFEMP1, HAPLN3, POSTN,* and *THBS1*, and regulators of ECM production and cell-ECM interactions such as *BMP2, GDF7,* and *FBLIM1*. Unlike the rest of the ECs, the valvular endothelium has low expression of HLA class II genes (*HLA-DRA, HLA-DRB1, HLA-DPA1*, etc.; Fig 2E, **S1 File in** S1 Data) or the invariant chain *CD74*, indicating a more immunologically neutral luminal surface. Importantly, valvular ECs seem more thromboresistant than the rest of the EC populations, since they overexpress *PTGS2* (also known as COX-2), the rate-limiting enzyme for prostacyclin biosynthesis (Fig 2E). Lastly, markers for lymphatic-like ECs include *CCL21, LYVE1, NR2F1, PDPN, PKHD1L1, PROX1, SEMA3A,* and *RELN* (S3A Fig), likely originating from lymphatic adventitial/periadventitial microvessels.

Intimal and medial SMCs: More similarities than differences

Smooth muscle cells represent 6.6 to 21.9% of cells in individual samples (Fig 1C) and a total of 2,298 cells in the focused UMAP (Fig 3A). Two main subpopulations of SMCs (*MYH11⁺DES^hi* SMC1, 532 cells; *MYH11⁺DES^lo* SMC2, 1248) and a cluster of pericyte-like cells (SMC3, 518 cells) were detected. The SMC1 and SMC2 clusters share transcriptional features in common that reflect a fully differentiated contractile phenotype. These include high expression of the contractile markers *ACTA2, MYH11, CALD1,* and *TAGLN*; contractile accessory proteins *TPM1, TPM2,* and *PPP1R14A*; actin polymerization and depolymerization factors *DSTN* and *LMOD1*; and moderate to high expression of the main TFs and cofactors responsible for these characteristics (*SRF, MYOCD, MRTFA, MRTFB, CSRP1*) (Fig 3, S6A and S6B Fig). The small number of differentially expressed genes between the SMC1 and SMC2 subclusters suggests that they represent distinct transcriptional states of the same population (S6A Fig). A summary of marker genes identifying SMC subclusters is presented in Table 1.

Immunofluorescence analyses confirmed the widespread localization of MYH11-positive SMCs in the intima and media. However, both venous SMC subclusters displayed transcriptional characteristics that could be associated with a potential for phenotypic modulation. For instance, the SMC1 population has transcriptional features associated with both increased contractility and enhanced migratory potential, a synthetic characteristic (Fig 3B–3D). Cells in this cluster show increased expression of the contractile markers *DES, CNN1, MYLK*, and the cold-induced adrenergic receptor *ADRA2C* (Fig 3B, S6A Fig) [42–44]. In parallel, they demonstrate significant upregulation of the β1 integrin subunit *ITGA5* and its ligand fibronectin
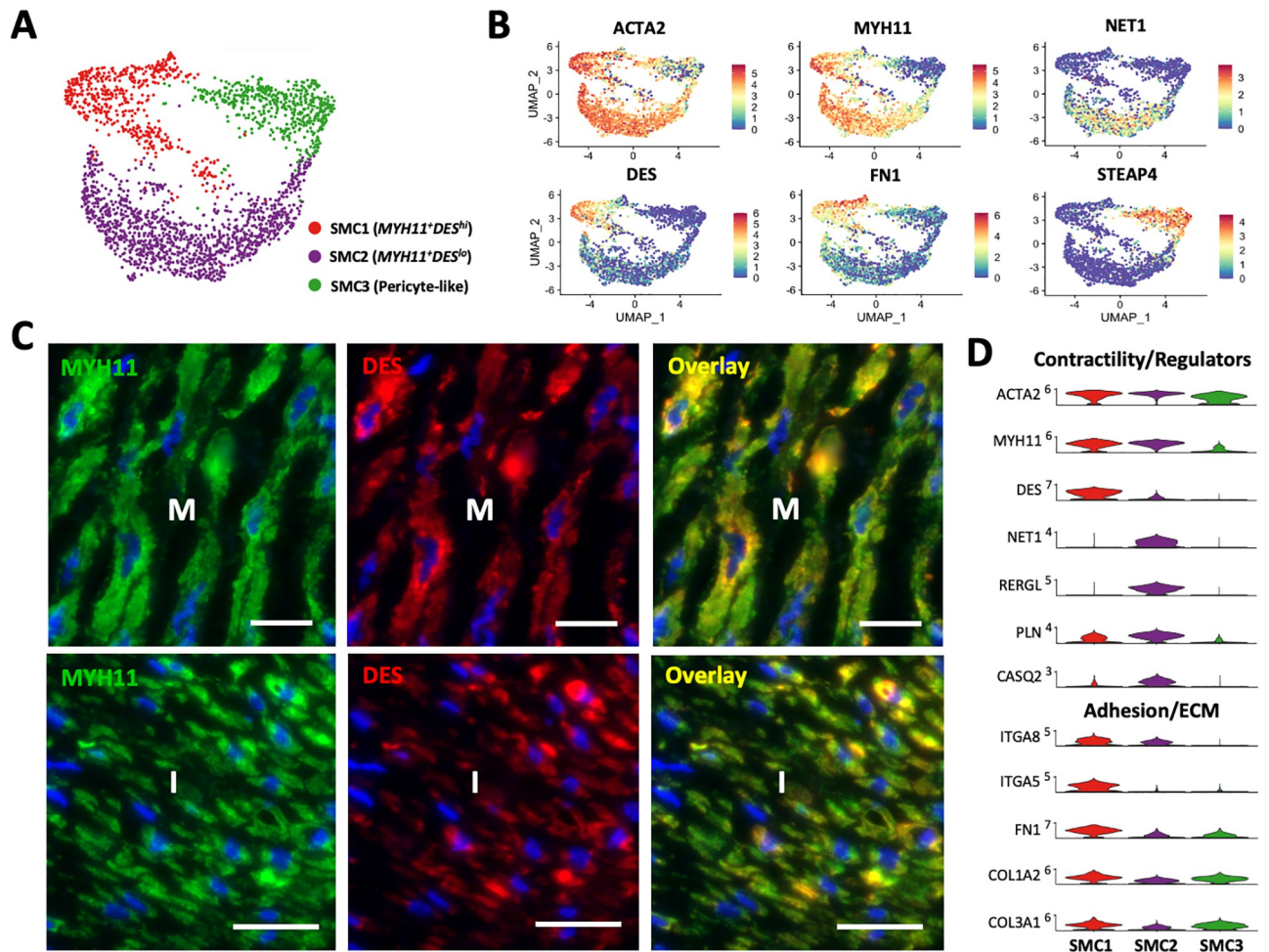
Fig 3. Smooth muscle cells (SMC) and pericytes in upper arm veins. A) Focused UMAP of 2,298 SMCs isolated from upper arm veins. **B)** Feature plots indicating normalized expression levels of markers characteristic of the 3 SMC populations. **C)** Localization of SMC1 ($MYH11^+DES^{hi}$) and SMC2 ($MYH11^+DES^{lo}$) cells in the intima (I) and media (M) by immunofluorescence. Scale bars represent 20 µm in all panels. **D)** Violin plot representation of expression differences among the 3 SMC populations.

https://doi.org/10.1371/journal.pone.0296264.g003

($FN1$), the F-actin stabilizing protein $PALLD$ [45], and the actin bundling protein $SYNPO2$, which further stabilizes lamellipodia and actin projections required for migration [46]. Upregulation of $ITGA5$ is associated with a synthetic phenotype in arterial SMCs, as well as connexin 43 ($GJA1$) and versican ($VCAN$), which are also upregulated in the $MYH11^+DES^{hi}$ SMC1 cluster (**S3 File in** S1 Data) [44, 47]. Our analyses reveal that $ITGA5^{hi}$ and DES^{hi} SMCs inhabit the intima and media irrespective of spindle-like or rounded morphologies (Fig 3C, S7A and S7B Fig). Upregulation of $FN1$, $COL1A2$, and $COL3A1$ in the SMC1 cluster may also explain the extensive deposition of ECM in the media of veins (Fig 3D, S1B Fig) and propensity of these cells for phenotypic modulation [48, 49].

Interestingly, $MYH11^+DES^{lo}$ SMC2 cells show increased expression of distinct regulators of the cell cytoskeleton and contractile machinery, such as the sarcoplasmic reticulum Ca-ATPase inhibitor PLN, the cytoskeletal adaptor protein $SORBS2$, the Rho guanine exchange factor (and RhoA activating protein) $NET1$, and the GDP/GTP binding protein $RERGL$ [42] (Fig 3D, S6A Fig). Activation of RhoA signaling can promote both the contractile and

synthetic phenotypes depending on the ECM [50]. Enrichment of the laminin receptor *BCAM* in SMC2 cells may contribute to the differentiated SMC phenotype by enhancing interactions with the basement membrane [51, 52]. In addition, highly expressed metalloproteinases such as *ADAMTS4* and *ADAMTS9* also allow focal adhesion turnover and control cell proliferation [53]. Gene ontology analyses predict a suppression of calcium ion transport due to upregulation of *PLN* and *CASQ2*, which may affect contractility (S5B Fig). A balance in expression of negative and positive regulators of smooth muscle contraction such as *HRH2* and *ADRA2A*, respectively, further support this scenario. Transcriptional regulators with higher levels in this population include the SRF cofactor *CSRP2*, *NOTCH3*, *PPARG* and its co-stimulatory factor *ADIRF*, and the myogenic differentiation gene *MUSTN1* (S6B Fig, **S3 File in** S1 Data) [54]. A higher proportion of SMC2 cells presents upregulation of *IL6* ($\geq$1 normalized copy) compared to the SMC1 cluster (240/1248, 19.2% vs. 21/532, 3.9%, respectively), indicating increased pro-inflammatory potential. Furthermore, upregulation of mitochondrial protein *NDUFA4L2* may represent an advantageous metabolic adaptation to low oxygen tension [55]. Immuno-localization analyses demonstrate that SMC2 cells co-exist in the intima and media with the SMC1 population, further supporting a migration-permissive environment in the wall irrespective of phenotypic characteristics. Cell-to-cell interactome analysis identified SMC2 cells as the main producers of placental growth factor (*PGF*) in the vein, with predicted paracrine effects on *FLT1* (VEGFR1)-expressing ECs and monocytes/macrophages (S6C Fig). Triggers of PGF secretion by SMCs include angiotensin II [56] and EC-derived reactive oxygen species in response to shear stress [57]. PGF is an angiogenic factor that promotes monocyte activation and recruitment to the endothelium [58–60].

Pericytes are supportive cells embedded within the endothelial basement membrane of VV microvessels (S7C Fig) with important roles in hemostasis and vascular infiltration [61]. The pericyte (SMC3) population identified in this study (defined by *STEAP4*, *APOE*, *CD36*, *EDNRB*, *CYGB*) is most closely related to the SMC2 cluster as indicated by pseudotime trajectory analysis (S6A and S6B Fig). From the transcriptional regulation standpoint, pericytes share expression of *SRF*, *MRTFA*, and *MRTFB* with the rest of the SMCs but lack *MYOCD*. The former also show upregulation of *NOTCH3*, *PPARG* and *TBX2* similar to SMC2 cells, but significantly higher levels of *NR2F2* compared to both SMC populations (S6B Fig, **S2 File in** S1 Data). Unique genes expressed in pericytes highlight the contribution of these cells to vascular maintenance, hemostasis, and inflammation. Upregulation of endothelin receptor type B (*EDNRB*) and cytoglobin (*CYGB*) supports their role in regulating microvessel diameter and oxygen diffusion. The combination of *CD36*, *APOE*, *STEAP4*, and *FABP4* indicates a cellular phenotype primed for lipid uptake and metabolism; whereas *THY1* is a cell surface ligand that supports leukocyte infiltration (S6A Fig, **S2 File in** S1 Data) [62].

Fibroblasts as regulators of EC survival and SMC proliferation

The proportions of fibroblasts ranged from 14.0 to 46.9% across the 4 veins analyzed (Fig 1C), for a total of 9,172 cells out of 20,006 in the focused UMAP (Fig 4A), and more than 4X the SMC count in these tissues. Immunohistochemistry (IHC) analyses of PDGFRA, a marker in common for all venous fibroblasts, underscored their abundance and widespread distribution in the wall. Specifically, they contribute to the population of intimal cells; they are found interspersed among SMC bundles in the media, and among elastic fibers in the adventitia (Fig 4B, S8A Fig). Their presence in the intima and media also suggests an important contribution to chronic wall remodeling, even in the absence of vascular injury. Venous fibroblasts subdivided into three main subclusters (activated, maintenance, and secretory), named according to their expression of myofibroblast markers, core ECM genes, and complement/adipogenic factors,
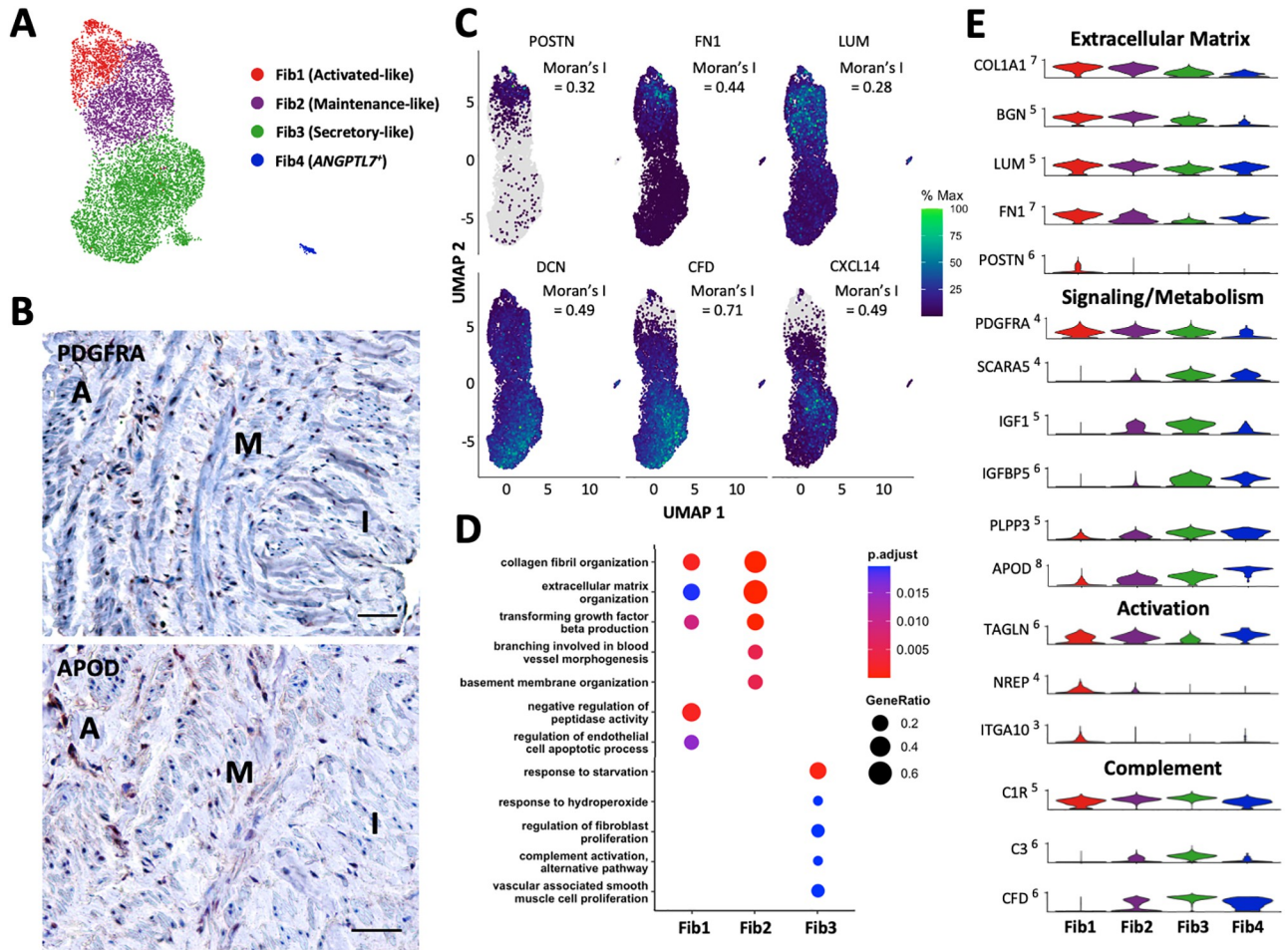
Fig 4. Fibroblasts in upper arm veins. A) Focused UMAP of 9,172 fibroblasts isolated from upper arm veins. **B)** Localization of PDGFRA+ (pan-fibroblast marker) and APOD+ (secretory marker) fibroblasts by immunohistochemistry. Scale bars represent 50 μm. **C)** Feature plots indicating the relative expressions of fibroblast markers across a pseudotime defined by transcriptional similarities among cells. The Moran's I statistics of spatial autocorrelation is shown for each gene. **D)** Gene ontology pathways unique and in common among the 3 main fibroblast subtypes. **E)** Violin plot representation of expression differences among fibroblast populations.

respectively. Separation into these subsets was mainly done to facilitate their phenotypic characterization (Table 1), but in reality, they organized following opposing gradients of ECM gene expression and secretory factor levels (Moran's I > 0.28, padj<0.001) as demonstrated by pseudotime trajectory analyses (Fig 4C).

Both activated (1,637 cells) and maintenance fibroblasts (2,073 cells) showed upregulation of collagens, proteoglycans, and other ECM proteins and regulators (*COL1A1, COL1A2, COL3A1, BGN, TNC, LUM, TIMP1*) compared to the secretory subset (Fig 4C–4E). They also overexpressed the adipogenic receptor *CDH13*, the vasoconstrictive receptor *CMKLR1*, the thrombin receptor *F2R*, and as in the case of SMC2 cells, *NDUFA4L2*, a component of the mitochondrial electron transport chain associated with adaptation to hypoxic conditions (**S4 File in** S1 Data). In addition, expression of *DKK3* and *MICAL2* suggests a baseline propensity for myofibroblastic activation as a result of additional cellular or mechanical stressors [63, 64]. This phenotypic transition was already observed in the activated fibroblast cluster, which were transcriptionally related to SMC1 cells by pseudotime analysis (S8C Fig). It is also possible that

activated fibroblasts represent a synthetic SMC population. The former display significant upregulation of *ACTA2*, *TAGLN*, *FN1*, the collagen-binding integrin subunit *ITGA10*, the co-activator of TGFβ translation *NREP* [65], and exclusive expression of periostin (*POSTN*) with respect to other fibroblasts (Fig 4E, **S4 File in** S1 Data). In terms of TFs, activated and maintenance fibroblasts share expression of *NOTCH3* with SMCs and pericytes, and of *FOXC2* with the latter populations and the valvular and lymphatic EC subclusters.

The most numerous fibroblast population, termed secretory fibroblasts (5,462 cells), was characterized by upregulation of complement factors (*C1S*, *C1R*, *C3*, *CFD*), angiogenesis regulators (*CD34*, *CXCL14*, *SFRP1*, *SVEP1*), and hemostatic proteins (*ACKR3*, *PTGDS*) compared to the above fibroblast subsets (Fig 4E, **S4 File in** S1 Data). High expression of genes related to adipocytic differentiation (*SCARA5*), lipid metabolism (*IGF1*, *IGFBP5*, *PLA2G2A*, *PLPP3*), and particularly, reduction of lipid peroxidation (*GPX3*, *MGST1*), suggests a role of secretory fibroblasts in lipid scavenging and detoxification. While they do not have high expression of ECM proteins, they do express genes that promote fibrotic remodeling (*CILP*, *PI16*, *CXCL14*). This secretory population, characterized by high *APOD* expression, was also widely distributed throughout the wall (Fig 4B, S8B Fig). Lastly, a small *ANGPTL7*+ fibroblast population (284 cells; Fig 4A) with potential pro-fibrotic effects [66] was detected in agreement with previous studies [6].

All three fibroblast phenotypes modulate EC and SMC function through cell-to-cell interactions. Specifically, angiopoietin-like factors (*ANGPTL1*, *ANGPTL2*) produced at different levels by the three fibroblasts are predicted to interact with ITGA5 expressing cells, to regulate EC survival, vascular permeability, promote proliferation and migration of medial SMCs, and increase immune cell infiltration (Figs 4D and 5) [66–69]. Upregulation of *IGFBP5* in SMCs is also expected to potentiate the effects of fibroblast-derived *IGF1* in inducing SMC proliferation (Fig 4D, S8D Fig) [70].

The venous endothelium is a niche for monocyte recruitment and infiltration

One of the most intriguing findings of our study is the high abundance of immune cells in healthy upper arm veins (Fig 1B and 1C, S9 Fig). There are a total of six immune subpopulations in the 4 veins analyzed, including 4931 monocytes/macrophages, 1165 T cells, 244 NK cells, 235 mast cells, and 142 neutrophils (Figs 1C, 6A and 6B). Monocytes/macrophages comprise the most prominent immune cluster, accounting for 18.3 to 43.8% of cells in samples. Counts of CD163+ monocyte/macrophages positively correlate with donor's age in histological sections (S9D Fig), which may explain the higher proportion of this cell cluster in samples BV1 and BV3 (Fig 1C). NK cells (0.5–2.5%), mast cells (0.4–1.3%), and neutrophils (0.3–1.9%) are found in smaller proportions. T lymphocytes (29.6% *CD8A*+, 7.6% *CD4*+) are present at low proportions in three of the veins (1.3–5.8%), but at 25.6% in the fourth one. Unlike monocyte/macrophages, there is no correlation between CD8+ cell counts by histology and donor's age (S9D Fig).

The overall monocyte/macrophage cluster can be identified by expression of CD14, CD16 (*FCGR3A*), CD163, and CD206 (*MRC1*) (Fig 6C). These further subdivided into two subclusters named according to other transcriptional features: Mo/Mφ1 (2,012 cells), which show upregulation of *IL1B*, *CCL20*, *CXCL3*, *CXCL8*, *TNF*, *EREG*, and the inflammasome sensor *NLRP3*; and Mo/Mφ2 (2,919 cells), a reparative phenotype that has been previously reported in non-vascular tissues [71–73]. The latter are characterized by high expression of *C1QA/B/C*, *FOLR2*, *HMOX1*, *LYVE1*, *RNASE1*, *SELENOP*, and *VSIG4* (Fig 6D and 6E, **S5 File in** S1 Data).
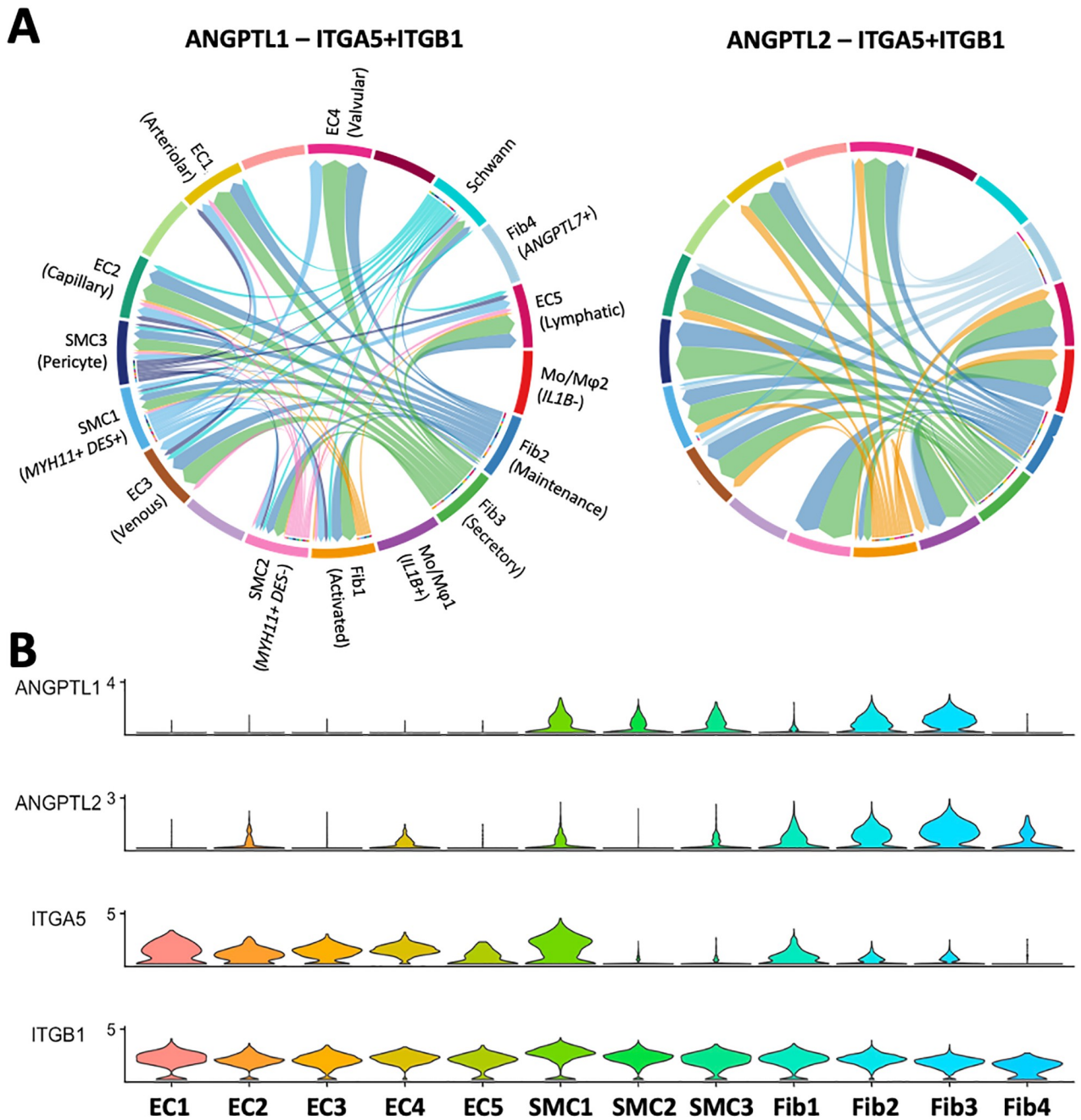
Fig 5. Regulation of ECs and SMCs by fibroblasts. A) Angiopoietin-like factors 1 and 2 secreted by maintenance, secretory, and *ANGPTL7+* fibroblasts regulate ITGA5-expressing ECs and SMC1 as predicted by CellChat ligand-receptor interactome analysis. Arrows inside bubbles indicate the direction of regulation, with the size of the incoming arrow representing the strength of the interaction. **B)** Expression levels of *ANGPTL1*, *ANGPTL2*, and the alpha (*ITGA5*) and beta (*ITGB1*) subunits of the integrin receptor in ECs, SMCs, and fibroblasts.

Along with CD163, this combination of genes is associated with hemoglobin and heme scavenging, apoptotic cell clearance (efferocytosis), and resolution of inflammation [74–76].

Both monocyte/macrophage phenotypes were the most important immune cells contributing to outgoing (ligand secretion) and incoming (receptor binding) interactions with other
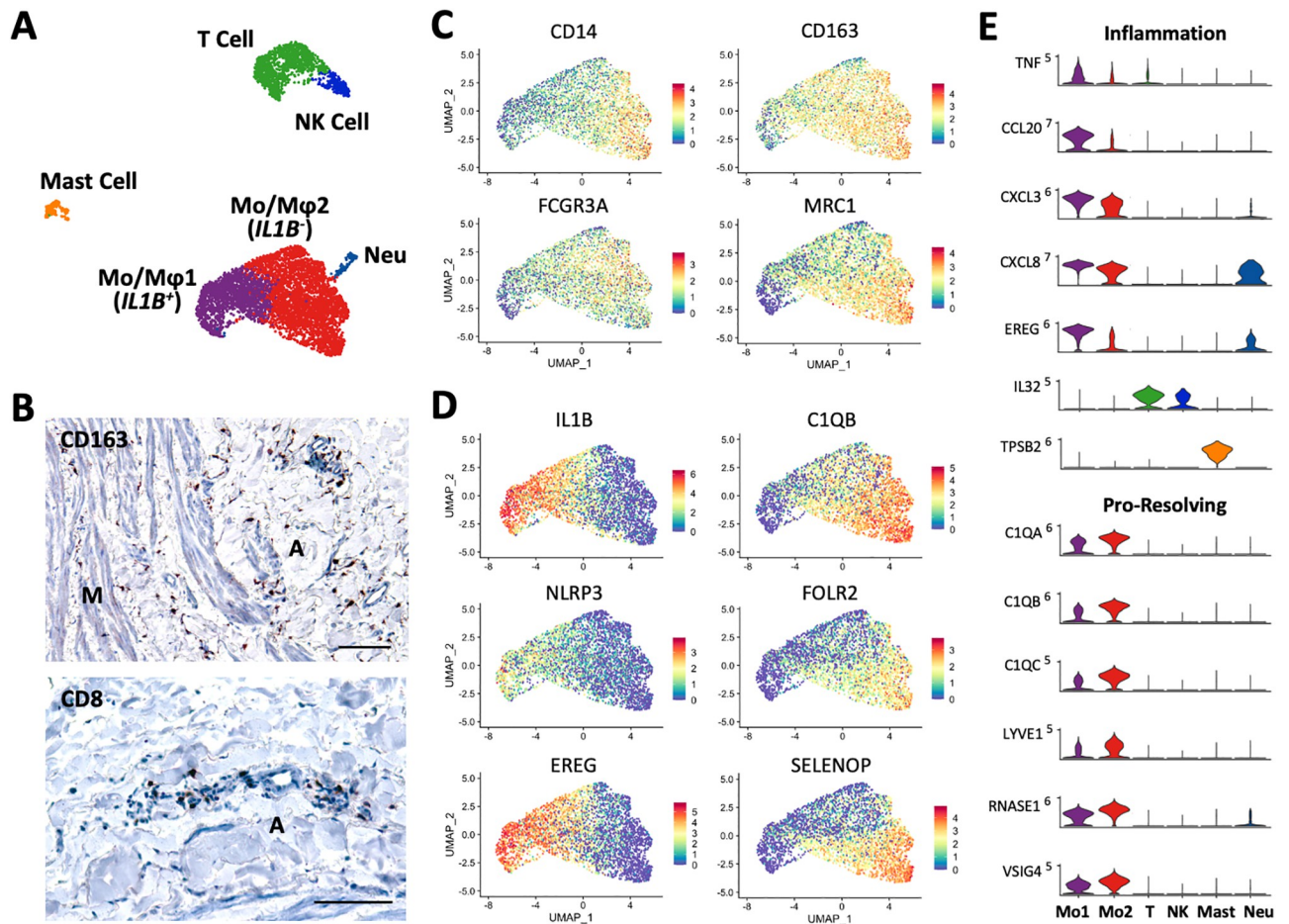
Fig 6. Immune cells in upper arm veins. A) Focused UMAP of 4931 monocytes/macrophages (Mo/Mφ), 1165 T cells, 244 NK cells, 235 mast cells, and 142 neutrophils (Neu) isolated from upper arm veins. **B)** Localization of CD163⁺ monocytes/macrophages and CD8⁺ T cells by immunohistochemistry. Scale bars represent 100 μm. **C-D)** Feature plots indicating normalized expression level of markers in common (C) and different (D) between the two monocyte/macrophage subpopulations. **E)** Violin plot representation of expression differences among immune cell populations.

https://doi.org/10.1371/journal.pone.0296264.g006

cells in the vascular wall (Fig 7A and 7B). Furthermore, GO analyses identified the pro-inflammatory Mo/Mφ1 population as the main immune cell type affecting survival, proliferation, and differentiation of ECs and SMCs (S9A Fig). Specifically, Mo/Mφ1-derived *IL1B* and *TNF* upregulate adhesion molecules, pro-inflammatory mediators, and pro-coagulant factors in ECs (Fig 7B, S9A Fig) [77–79]. Thrombospondin-1 (*THBS1*) produced by pro-inflammatory Mo/Mφ1 cells has anti-proliferative properties for ECs but positively regulates SMC proliferation and migration [80, 81]. Mo/Mφ1-derived epiregulin (*EREG*) is also a potent SMC mitogen (S9A Fig, **S5 File in** S1 Data) [82]. In addition to ECs and SMCs, Mo/Mφ1 cells promote survival of secretory fibroblasts through secretion of *CLCF1* and activation of the fibroblast *CNTFR* receptor (LIFR pathway in Fig 7B). Fibroblasts, in turn, are important regulators of macrophage function via secretion of complement factors and IL6. Both Mo/Mφ1 cells and venous ECs activate and increase survival of infiltrated neutrophils through production of *IL1* factors and *CSF3*, respectively (Fig 7B).

Venous ECs are specifically affected by macrophage-derived chemokines *CXCL1*, *2*, *3*, and *8* via activation of the ACKR1 receptor (Fig 7B–7D). Additional chemokines modulating
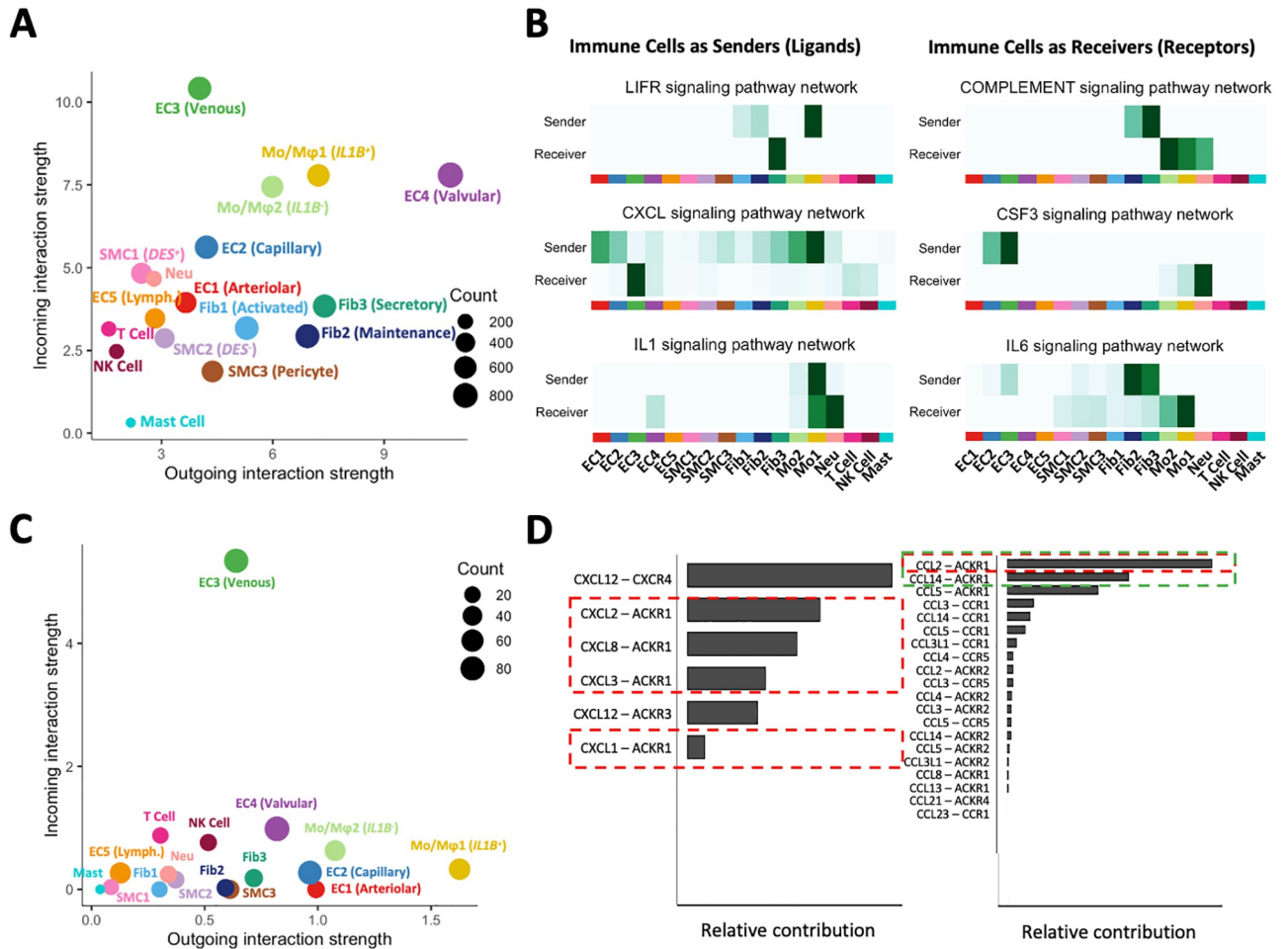
Fig 7. Ligand-receptor interactions among venous cell populations. A) Global plot of outgoing (ligand) and incoming (receptor) interactions among cell populations in veins as predicted by CellChat. Venous ECs are the top receivers among all populations. Valvular ECs are the top senders of signals. Monocytes/macrophages (Mo/Mφ) are the main immune populations participating as senders and receivers of global interactions. **B)** Examples of pathways where immune cells act as senders (left) or receivers (right) of signals. **C)** Plot of outgoing and incoming interactions among cell populations specifically for the chemokine (CXCL/CCL) signaling pathway. Venous ECs are the main receivers of signals through the ACKR1 receptor, while $IL1B^+$ Mo/Mφ are the top senders. **D)** Relative contribution of specific chemokines to the plot in C. Red boxes indicate chemokines secreted by $IL1B^+$ Mo/ Mφ, while the green box marks chemokines secreted by venous/capillary ECs (CCL14) or other cells including venous ECs (CCL2).

https://doi.org/10.1371/journal.pone.0296264.g007

venous ECs include *CCL2* from all cells except T and NK cells, *CCL14* from other venous and capillary-like ECs, and *CCL5* from T lymphocytes. Of note, regardless of the cellular origin of these cytokines and chemokines, the ability of ACKR1 to allow transcytosis suggests that the main lumen of veins and VV venules maintain a microenvironment that serves as beacon for monocytes. Immunohistochemistry analyses demonstrate that CD163$^+$ monocytes/macro-phages and CD8$^+$ T cells are abundant in the adventitia, particularly in the vicinity and lumen of microvessels (Fig 6B, S9B and S9C Fig).

Discussion

Peripheral veins are the preferred anatomical location for creation of vascular accesses for hemodialysis (arm veins) and common conduits for coronary bypass surgeries (saphenous vein). This single-cell transcriptomic study demonstrates for the first time that: 1) veins harbor

a cellular ecosystem of abundant fibroblasts and immune cells in much higher proportions than SMCs; 2) the existence of VV consisting of a complex populaton of ECs of various arterio-venous zonation phenotypes; 3) a unique transcriptional profile in venous SMCs; and 4) the widespread presence of regulatory, reparative, and interacting fibroblasts in all layers of the vascular wall. This granular knowledge of the cellular composition and transcriptional states of cells in human peripheral veins may lead to a better understanding of venous physiology and mechanisms underlying diseases and post-operative complications.

The heterogeneity of EC phenotypes as defined by arteriovenous zonation markers illustrates at the transcriptional level the ECs lining the intima, and the complex microvascular structures of VV irrigating the outer media and adventitia. The venous VV has been previously described with elegant 3D renderings of scanning electron microscopy [24], but little is known about this vascular network at the molecular level. The majority of ECs were of the venous type that histological located in the endothelial line of the lumen and the extensive network of draining venous VV [24], We also identified an abundant capillary EC population that went unnoticed in prior studies [25], and which may be important for expansion of the VV during postoperative remodeling or, in the case of lower extremities, for the development of chronic venous insufficiency. The high expression of adhesion molecules in venous ECs, upregulation of pro-inflammatory mediators, and ACKR1-mediated transcytosis of chemokines [83] redefine the concept of endothelial activation, and underscores the role of the main venous lumen and VV venules as preferential sites of infiltration and a niche for both reparative and pro-inflammatory immune cell populations.

We also demonstrated that SMCs in human veins are positive for *MYH11* and other markers of contractility, but have additional transcriptional features that challenge this arterial-based phenotypic classification. Synthetic SMCs in single-cell studies of arteries have been identified as having low expression of contractile genes such as *MYH11*, *ACTG*, and *CNN1* and high levels of ECM genes [1, 3, 10]. In contrast, two transcriptional states of $MYH11^+$ SMCs coinhabited the intima and media in veins, distinguished by upregulation of *DES* and *ITGA5* in one state and of RhoA signaling proteins in the other. Upregulation of *ITGA5*, fibronectin, and collagens by DES^{hi} SMCs supports an active ECM remodeling phenotype and high migratory and proliferative potential [48, 49]. On the other hand, DES^{lo} SMCs express genes associated with negative regulation of contractility and have higher pro-angiogenic and -inflammatory gene expression. Historically, the "contractile" phenotype has been defined by high expression of genes in the actomyosin apparatus (particularly *MYH11*) and location in the media, but not necessarily by functional assessment. Considering that the main function of veins is not contractility, that arms veins specifically have a negligible myogenic tone [84], and that contractile proteins also play crucial functions in cell migration [85], this "contractile" phenotype in veins calls for future investigations. Along these lines, the value of desmin as a contractile marker in bladder SMCs has been recently debated [86].

Stenotic remodeling and IH in veins are often associated with expansion of a synthetic SMC phenotype and migration of activated fibroblasts from the adventitia after vascular injury [16, 87]. Interestingly, we did not observe a clear transcriptomic distinction between medial and intimal SMCs, or between spindle-shaped or rounded SMC morphologies in these layers. Furthermore, there was a widespread distribution of fibroblasts in the walls of these veins, interspersed among SMCs in the intima and media. It is likely that in the absence of well formed internal and external elastic laminae, the structure of the vein is fully permissive to cell migration. Therefore, unlike arterial diseases, the cells contributing to venous IH may not need to dedifferentiate extensively or migrate from the adventitia. Phenotypic similarities between intimal and medial SMCs, their pro-remodeling transcriptional profiles, and the widespread distribution of fibroblasts may also explain the tendency of veins to chronically

develop IH and fibrosis [15]. Ultimately, comparative studies with veins obtained after vascular surgeries will be necessary to evaluate the true cellular contributors to postoperative IH and their molecular differentiation.

Lastly, cell-to-cell signaling underscored the versatility of venous fibroblasts in regulating immune cell populations, ECs, and SMCs through complement factors, pro-inflammatory mediators, and angiopoietin-like proteins. Like ECs, venous fibroblast phenotypes may contribute to perpetuating or resolving vascular inflammation. Secretory fibroblasts are also important regulators of intramural vascularization [88].

In conclusion, this study presents for the first time, to our knowledge, a detailed cellular atlas of upper arm veins with molecular information that is particularly relevant to the study of post-surgical venous remodeling after vascular access creation. Our data provide the groundwork for future molecular studies and single-cell characterizations of veins in the setting of vascular injury and patient comorbidities. We present compelling evidence of the venous endothelium as a preferential site of immune surveillance and infiltration, and of complex SMC/non-SMC interactions in the intima and media that may underlie clinical outcomes after vascular procedures.

Materials and methods

Sample collection and tissue processing

The study cohort included 16 organ donors whose tissues were donated for research through a collaboration with the Life Alliance Organ Recovery Agency (no informed consent required; S1 Table). Cross-sectional samples of upper arm vessels (12 basilic veins, 3 cephalic veins, 1 brachial artery), approximately 2 cm in length, were obtained *post mortem* following organ procurement procedures. For single-cell RNA sequencing, 4 veins (3 basilic, 1 cephalic) were collected in cold cell culture media cold for tissue dissociation (S1 File). The remaining 12 samples were collected in RNA*later* (QIAGEN, Germantown, MD) and stored at -80°C. A 5 mm cross-section was fixed in 10% neutral formalin (Sigma-Aldrich, St. Louis, MO) for paraffin embedding and sectioning.

Single-cell RNA sequencing and bioinformatic analyses

Single-cell RNA sequencing was performed in the Center for Genome Technology at the University of Miami John P. Hussman Institute for Human Genomics. Sequencing data were processed in R (4.2.2) using Seurat v4 and available packages for quality control (QC), integration, and bioinformatic inferences [89–95] as described in the S1 File. Briefly, a total of 31,109 cells were obtained after 10X droplet generation and single cell sequencing. For quality control (QC), we adjusted for ambient RNA contamination and filtered out predicted doublets and cells with >15% mitochondrial genes and <200 genes, resulting in 21,131 high quality cells for downstream analysis (S2A and S2B Fig). We then excluded clusters with less than 40 cells and those defined by markers of cell division (*CENPF*, *MKI67*, *TOP2A*; 697 cells). The integrated map was generated using the package Harmony [92]. Sequencing data have been deposited in the Gene Expression Omnibus (GEO), accession number GSE250469.

Histology and immunohistochemistry analyses

Tissue sections were stained with Masson's (Polysciences #25088–1) trichrome and Movat's pentachrome (Abcam #ab245884) for gross histomorphometric analysis. For IHC and IF, specific proteins were detected using the primary antibodies and methodology described in the S1 File.

Supporting information

S1 Table. Demographic characteristics of the single-cell RNA sequencing and histological validation cohorts.
(PDF)

S1 Fig. Histology of upper arm vessels. Representative Movat pentachrome stained sections of vascular tissues used for validation studies. Images include three basilic veins (**A**), two cephalic veins (**B**) and a brachial artery as reference (**C**). Dashed boxes are magnified to the right.
(PDF)

S2 Fig. Quality control (QC) metrics of single-cell RNA libraries. A) Number of genes versus number of UMIs (transcripts) per cell after initial QC filters with color legend indicating mitochondrial read fractions (mitoRatio). **B)** Cell density histograms indicating distribution of UMI counts and gene counts per cell in the four vein samples. Cells with <200 genes, >0.15 mitoRatio, or predicted as doublets were filtered out from downstream bioinformatic analyses. **C)** UMAP plot color coded by sample demonstrating cell integration of individual single cell libraries.
(PDF)

S3 Fig. Transcriptional profiling of endothelial cell (EC) populations in veins. A) Heatmap of single-cell gene expression data for the top differentially expressed genes among EC subclusters in veins. Genes are shown in rows and cells in columns, color-coded according to the main arteriovenous zonation phenotypes (EC1: arteriolar-like, EC2: capillary-like, EC3: venous-like, EC4: valvular-like, and EC5: lymphatic-like). **B)** Feature plots indicating the relative expressions of transcription factors and ephrinB2 ligand and receptor markers across a pseudotime defined by arteriovenous zonation phenotypes. The pseudotime direction goes from EC1 to EC4 followed by EC5, with the Moran's I statistics of spatial autocorrelation shown for each gene. **C)** Gene expression levels of positive (*SNAI1*) and negative regulators (*EPB41L3*) of endothelial to mesenchymal transition in the five EC subclusters.
(PDF)

S4 Fig. Venous endothelial cells in the lumen and vasa vasorum. A) Representative co-immunofluorescence of the venous EC markers PLVAP and ACKR1 in the main lumen (left) and venous vasa vasorum (right). The yellow color indicates colocalization of both markers in the lumen and venules. **B)** Co-immunofluorescence of PLVAP and GJA5 in the main lumen (left) and vasa vasorum (right). There is low protein expression of GJA5 in the lumen and venules, while localization of GJA5 and PLVAP discriminates between arterioles (Art.) and venules (Ven.) in the vasa vasorum. Scale bars represent 20 μm in all panels.
(PDF)

S5 Fig. Predicted functional differences among cell populations in veins. Gene ontology pathway analysis of genes expressed in endothelial cell (**A**) and smooth muscle cell (**B**) populations in veins. EC1: arteriolar-like, EC2: capillary-like, EC3: venous-like, EC4: valvular-like, EC5: lymphatic-like, SMC1: $MYH11^+DES^{hi}$, SMC2: $MYH11^+DES^{lo}$, SMC3: pericyte-like.
(PDF)

S6 Fig. Transcriptional profiling of smooth muscle cell (SMC) populations in veins. A) Heatmap of single-cell gene expression data for the top differentially expressed genes among SMC subclusters in veins. Genes are shown in rows and cells in columns, color-coded by subcluster (SMC1: $MYH11^+DES^{hi}$, SMC2: $MYH11^+DES^{lo}$, and SMC3: pericyte-like). **B)** Feature plots indicating the relative expressions of transcription factors across a pseudotime defined

by transcriptional similarities among cells. The pseudotime direction goes from SMC1 to SMC3, with the Moran's I statistics of spatial autocorrelation shown for each gene. **C)** The SMC2 population is the main source of placental growth factor (*PGF*) in the vein with pro-angiogenic effects on *FLT1*-expressing EC1, EC2, EC3, and pro-inflammatory monocyte/macrophages, as predicted by CellChat ligand-receptor interactome analysis. Arrows in the bubble indicate the direction of regulation, with the size of the incoming arrow representing the strength of the interaction.
(PDF)

S7 Fig. Types of smooth muscle cells in veins. A) Representative co-immunofluorescence of MYH11 and desmin in medial (left) and intimal SMCs (right). Cells with high (yellow-orange) and low desmin expression (green) coexist in both layers. **B)** Co-immunofluorescence of MYH11 and ITGA5 in medial (left) and intimal SMCs (right) shows similar distribution of ITGA5 high and low cells as in **A**. **C)** STEAP4+ pericytes surrounding microvessels. Scale bar = 20 μm in all panels.
(PDF)

S8 Fig. Venous fibroblasts. A) Representative IHC of PDGFRA[+] fibroblasts in veins demonstrates widespread distribution in the wall. Scale bars = 50 μm. **B)** Immunofluorescence of APOD in the intima (I), media (M), and adventitia (A). APOD[+] fibroblasts appear in pink while extracellular APOD is shown in red. Scale bars = 20 μm. **C)** The Fib1 cluster is most closely related to SMC1 cells as predicted by pseudotime trajectory analysis. **D)** *IGFBP5* in SMCs can potentiate the effects of insulin-like growth factor 1 (*IGF1*) from fibroblasts to promote SMC proliferation.
(PDF)

S9 Fig. Immune cells in veins. A) Gene ontology pathway analysis of genes expressed in immune cell populations in veins. Mo: monocyte/macrophages, NK: natural killer cells, Mast: mast cells, Neu: neutrophils. **B-C)** Representative stainings of CD163^{+} monocyte/macrophages (**B**) and CD8^{+} T cells (**C**) in basilic veins from the validation cohort. Scale bars represent 50 μm in all panels. A: adventitia, M: media. D) Donor's age is positively correlated with CD163^{+} cell counts, but not CD8^{+} counts, in 6–7 basilic veins analyzed by IHC.
(PDF)

S1 File. Detailed methodology of sample collection, tissue processing, single-cell RNA sequencing, bioinformatic pipelines, and histological validations.
(PDF)

S1 Data. Cell population markers. Cell markers and gene expression differences among endothelial cell (S1), smooth muscle cell (S2-S3), fibroblast (S4), and immune cell (S5) subpopulations as determined by Wilcoxon signed ranks tests.
(XLSX)

Acknowledgments

Author Contributions

Conceptualization: Roberto I. Vazquez-Padron, Laisel Martinez.

Data curation: Miguel G. Rojas, Zachary M. Zigmond, Christina Kosanovic, Anthony J. Griswold, Roberto I. Vazquez-Padron, Laisel Martinez.

Formal analysis: Miguel G. Rojas, Zachary M. Zigmond, Roberto I. Vazquez-Padron, Laisel Martinez.

Funding acquisition: Roberto I. Vazquez-Padron, Laisel Martinez.

Investigation: Miguel G. Rojas, Zachary M. Zigmond, Simone Pereira-Simon, Nieves Santos Falcon, Maya Suresh Kumar, Filipe F. Stoyell-Conti, Anthony J. Griswold, Alghidak Salama, Xiaofeng Yang, Marwan Tabbara, Roberto I. Vazquez-Padron, Laisel Martinez.

Methodology: Miguel G. Rojas, Zachary M. Zigmond, Simone Pereira-Simon, Nieves Santos Falcon, Maya Suresh Kumar, Filipe F. Stoyell-Conti, Christina Kosanovic, Anthony J. Griswold, Roberto I. Vazquez-Padron, Laisel Martinez.

Project administration: Roberto I. Vazquez-Padron, Laisel Martinez.

Resources: Alghidak Salama, Xiaofeng Yang, Marwan Tabbara, Roberto I. Vazquez-Padron, Laisel Martinez.

Software: Miguel G. Rojas, Christina Kosanovic, Anthony J. Griswold, Roberto I. Vazquez-Padron, Laisel Martinez.

Supervision: Anthony J. Griswold, Alghidak Salama, Marwan Tabbara, Roberto I. Vazquez-Padron, Laisel Martinez.

Validation: Zachary M. Zigmond, Maya Suresh Kumar, Roberto I. Vazquez-Padron, Laisel Martinez.

Visualization: Miguel G. Rojas, Zachary M. Zigmond, Nieves Santos Falcon, Maya Suresh Kumar, Roberto I. Vazquez-Padron, Laisel Martinez.

Writing – original draft: Miguel G. Rojas, Roberto I. Vazquez-Padron, Laisel Martinez.

Writing – review & editing: Miguel G. Rojas, Zachary M. Zigmond, Simone Pereira-Simon, Nieves Santos Falcon, Maya Suresh Kumar, Filipe F. Stoyell-Conti, Christina Kosanovic, Anthony J. Griswold, Alghidak Salama, Xiaofeng Yang, Marwan Tabbara, Roberto I. Vazquez-Padron, Laisel Martinez.

References

1. Hu Z, Liu W, Hua X, Chen X, Chang Y, Hu Y, et al. Single-Cell Transcriptomic Atlas of Different Human Cardiac Arteries Identifies Cell Types Associated With Vascular Physiology. Arterioscler Thromb Vasc Biol. 2021; 41(4):1408–27. https://doi.org/10.1161/ATVBAHA.120.315373 PMID: 33626908

2. Wirka RC, Wagh D, Paik DT, Pjanic M, Nguyen T, Miller CL, et al. Atheroprotective roles of smooth muscle cell phenotypic modulation and the TCF21 disease gene as revealed by single-cell analysis. Nat Med. 2019; 25(8):1280–9. https://doi.org/10.1038/s41591-019-0512-5 PMID: 31359001

3. Crnkovic S, Valzano F, Fliesser E, Gindlhuber J, Thekkekara Puthenparampil H, Basil M, et al. Single-cell transcriptomics reveals skewed cellular communication and phenotypic shift in pulmonary artery remodeling. JCI Insight. 2022; 7(20). https://doi.org/10.1172/jci.insight.153471 PMID: 36099047

4. Fernandez DM, Rahman AH, Fernandez NF, Chudnovskiy A, Amir ED, Amadori L, et al. Single-cell immune landscape of human atherosclerotic plaques. Nat Med. 2019; 25(10):1576–88. https://doi.org/10.1038/s41591-019-0590-4 PMID: 31591603

5. Depuydt MAC, Prange KHM, Slenders L, Ord T, Elbersen D, Boltjes A, et al. Microanatomy of the Human Atherosclerotic Plaque by Single-Cell Transcriptomics. Circ Res. 2020; 127(11):1437–55. https://doi.org/10.1161/CIRCRESAHA.120.316770 PMID: 32981416

6. Sun Y, Hu X, Zhang K, Rao M, Yin P, Dong R. A Single-Cell Survey of Cellular Heterogeneity in Human Great Saphenous Veins. Cells. 2022; 11(17). https://doi.org/10.3390/cells11172711 PMID: 36078120

7. Martinez L, Rojas MG, Tabbara M, Pereira-Simon S, Santos Falcon N, Rauf MA, et al. The transcriptomics of the human vein transformation after arteriovenous fistula anastomosis uncovers layer-specific remodeling and hallmarks of maturation failure. Kidney Int Rep. 2023. https://doi.org/10.1016/j.ekir.2023.01.008 PMID: 37069981

8. Tisato V, Zauli G, Voltan R, Gianesini S, di Iasio MG, Volpi I, et al. Endothelial cells obtained from patients affected by chronic venous disease exhibit a pro-inflammatory phenotype. PloS one. 2012; 7 (6):e39543. https://doi.org/10.1371/journal.pone.0039543 PMID: 22737245

9. Chou EL, Chaffin M, Simonson B, Pirruccello JP, Akkad AD, Nekoui M, et al. Aortic Cellular Diversity and Quantitative Genome-Wide Association Study Trait Prioritization Through Single-Nuclear RNA Sequencing of the Aneurysmal Human Aorta. Arterioscler Thromb Vasc Biol. 2022; 42(11):1355–74. https://doi.org/10.1161/ATVBAHA.122.317953 PMID: 36172868

10. Pedroza AJ, Tashima Y, Shad R, Cheng P, Wirka R, Churovich S, et al. Single-Cell Transcriptomic Profiling of Vascular Smooth Muscle Cell Phenotype Modulation in Marfan Syndrome Aortic Aneurysm. Arterioscler Thromb Vasc Biol. 2020; 40(9):2195–211. https://doi.org/10.1161/ATVBAHA.120.314670 PMID: 32698686

11. Davis FM, Tsoi LC, Ma F, Wasikowski R, Moore BB, Kunkel SL, et al. Single-cell Transcriptomics Reveals Dynamic Role of Smooth Muscle Cells and Enrichment of Immune Cell Subsets in Human Abdominal Aortic Aneurysms. Ann Surg. 2022; 276(3):511–21. https://doi.org/10.1097/SLA.0000000000005551 PMID: 35762613

12. Maya ID, Oser R, Saddekni S, Barker J, Allon M. Vascular access stenosis: comparison of arteriovenous grafts and fistulas. Am J Kidney Dis. 2004; 44(5):859–65. PMID: 15492952

13. Harskamp RE, Lopes RD, Baisden CE, de Winter RJ, Alexander JH. Saphenous vein graft failure after coronary artery bypass surgery: pathophysiology, management, and future directions. Ann Surg. 2013; 257(5):824–33. https://doi.org/10.1097/SLA.0b013e318288c38d PMID: 23574989

14. Martinez L, Duque JC, Tabbara M, Paez A, Selman G, Hernandez DR, et al. Fibrotic Venous Remodeling and Nonmaturation of Arteriovenous Fistulas. J Am Soc Nephrol. 2018; 29(3):1030–40. https://doi.org/10.1681/ASN.2017050559 PMID: 29295872

15. Labissiere X, Zigmond ZM, Challa A, Montoya C, Manzur-Pineda K, Abraham A, et al. Vein morphometry in end-stage kidney disease: Teasing out the contribution of age, comorbidities, and vintage to chronic wall remodeling. Front Cardiovasc Med. 2022; 9:1005030. https://doi.org/10.3389/fcvm.2022.1005030 PMID: 36419492

16. Vazquez-Padron RI, Duque JC, Tabbara M, Salman LH, Martinez L. Intimal Hyperplasia and Arteriovenous Fistula Failure: Looking Beyond Size Differences. Kidney360. 2021; 2(8):1360–72. https://doi.org/10.34067/KID.0002022021 PMID: 34765989

17. Davies AH, Magee TR, Baird RN, Sheffield E, Horrocks M. Pre-bypass morphological changes in vein grafts. Eur J Vasc Surg. 1993; 7(6):642–7. https://doi.org/10.1016/s0950-821x(05)80710-8 PMID: 8270066

18. Wali MA, Eid RA, Dewan M, Al-Homrany MA. Intimal changes in the cephalic vein of renal failure patients before arterio-venous fistula (AVF) construction. J Smooth Muscle Res. 2003; 39(4):95–105. https://doi.org/10.1540/jsmr.39.95 PMID: 14692695

19. Kirsch D, Dienes HP, Kuchle R, Duschner H, Wahl W, Bottger T, et al. Changes in the extracellular matrix of the vein wall—the cause of primary varicosis? Vasa. 2000; 29(3):173–7. https://doi.org/10.1024/0301-1526.29.3.173 PMID: 11037714

20. Xu Y, Bian X, Chu H, Zhao J, Wang T, Tang J, et al. Effects of high hemodynamics upon the morphology of the walls of the great saphenous vein and splenic vein. Int Angiol. 2014; 33(3):292–8. PMID: 24936536

21. Wali MA, Eid RA, Al-Homrany MA. Smooth muscle changes in the cephalic vein of renal failure patients before use as an arteriovenous fistula (AVF). J Smooth Muscle Res. 2002; 38(3):75–85. https://doi.org/10.1540/jsmr.38.75 PMID: 12596887

22. Wali MA, Eid RA. Changes of elastic and collagen fibers in varicose veins. Int Angiol. 2002; 21(4):337–43. PMID: 12518113

23. Cocciolone AJ, Hawes JZ, Staiculescu MC, Johnson EO, Murshed M, Wagenseil JE. Elastin, arterial mechanics, and cardiovascular disease. Am J Physiol Heart Circ Physiol. 2018; 315(2):H189–H205. https://doi.org/10.1152/ajpheart.00087.2018 PMID: 29631368

24. Herbst M, Holzenbein TJ, Minnich B. Characterization of the vasa vasorum in the human great saphenous vein: a scanning electron microscopy and 3D-morphometry study using vascular corrosion casts. Microsc Microanal. 2014; 20(4):1120–33. https://doi.org/10.1017/S1431927614001287 PMID: 24913662

25. Duque JC, Martinez L, Tabbara M, Parikh P, Paez A, Selman G, et al. Vascularization of the arteriovenous fistula wall and association with maturation outcomes. J Vasc Access. 2020; 21(2):161–8. https://doi.org/10.1177/1129729819863584 PMID: 31608758

26. Loesch A, Dashwood MR. Vasa vasorum inside out/outside in communication: a potential role in the patency of saphenous vein coronary artery bypass grafts. J Cell Commun Signal. 2018; 12(4):631–43. https://doi.org/10.1007/s12079-018-0483-1 PMID: 30078142

27. Baklanov DV, Peters KG, Seidel AL, Taylor DA, Annex BH. Neovascularization in intimal hyperplasia is associated with vein graft failure after coronary artery bypass surgery. Vasc Med. 2003; 8(3):163–7. https://doi.org/10.1191/1358863x03vm488oa PMID: 14989556

28. He Y, Tacconi C, Dieterich LC, Kim J, Restivo G, Gousopoulos E, et al. Novel Blood Vascular Endothe-lial Subtype-Specific Markers in Human Skin Unearthed by Single-Cell Transcriptomic Profiling. Cells. 2022; 11(7). https://doi.org/10.3390/cells11071111 PMID: 35406678

29. Schupp JC, Adams TS, Cosme C Jr., Raredon MSB, Yuan Y, Omote N, et al. Integrated Single-Cell Atlas of Endothelial Cells of the Human Lung. Circulation. 2021; 144(4):286–302. https://doi.org/10.1161/CIRCULATIONAHA.120.052318 PMID: 34030460

30. Winkler EA, Kim CN, Ross JM, Garcia JH, Gil E, Oh I, et al. A single-cell atlas of the normal and mal-formed human brain vasculature. Science. 2022; 375(6584):eabi7377. https://doi.org/10.1126/science.abi7377 PMID: 35084939

31. Mellor RH, Brice G, Stanton AW, French J, Smith A, Jeffery S, et al. Mutations in FOXC2 are strongly associated with primary valve failure in veins of the lower limb. Circulation. 2007; 115(14):1912–20. https://doi.org/10.1161/CIRCULATIONAHA.106.675348 PMID: 17372167

32. Wang HU, Chen ZF, Anderson DJ. Molecular distinction and angiogenic interaction between embryonic arteries and veins revealed by ephrin-B2 and its receptor Eph-B4. Cell. 1998; 93(5):741–53. https://doi.org/10.1016/s0092-8674(00)81436-1 PMID: 9630219

33. Gerety SS, Wang HU, Chen ZF, Anderson DJ. Symmetrical mutant phenotypes of the receptor EphB4 and its specific transmembrane ligand ephrin-B2 in cardiovascular development. Mol Cell. 1999; 4 (3):403–14. https://doi.org/10.1016/s1097-2765(00)80342-1 PMID: 10518221

34. Protack CD, Foster TR, Hashimoto T, Yamamoto K, Lee MY, Kraehling JR, et al. Eph-B4 regulates adaptive venous remodeling to improve arteriovenous fistula patency. Sci Rep. 2017; 7(1):15386. https://doi.org/10.1038/s41598-017-13071-2 PMID: 29133876

35. Diehl S, Bruno R, Wilkinson GA, Loose DA, Wilting J, Schweigerer L, et al. Altered expression patterns of EphrinB2 and EphB2 in human umbilical vessels and congenital venous malformations. Pediatr Res. 2005; 57(4):537–44. https://doi.org/10.1203/01.PDR.0000155761.70710.C4 PMID: 15718372

36. Li Q, Zhu Z, Wang L, Lin Y, Fang H, Lei J, et al. Single-cell transcriptome profiling reveals vascular endothelial cell heterogeneity in human skin. Theranostics. 2021; 11(13):6461–76. https://doi.org/10.7150/thno.54917 PMID: 33995668

37. Thiriot A, Perdomo C, Cheng G, Novitzky-Basso I, McArdle S, Kishimoto JK, et al. Differential DARC/ACKR1 expression distinguishes venular from non-venular endothelial cells in murine tissues. BMC Biol. 2017; 15(1):45. https://doi.org/10.1186/s12915-017-0381-7 PMID: 28526034

38. Bosma EK, van Noorden CJF, Schlingemann RO, Klaassen I. The role of plasmalemma vesicle-associ-ated protein in pathological breakdown of blood-brain and blood-retinal barriers: potential novel thera-peutic target for cerebral edema and diabetic macular edema. Fluids Barriers CNS. 2018; 15(1):24. https://doi.org/10.1186/s12987-018-0109-2 PMID: 30231925

39. Yuan X, Piao L, Wang L, Han X, Tong L, Shao S, et al. Erythrocyte membrane protein band 4.1-like 3 inhibits osteosarcoma cell invasion through regulation of Snai1-induced epithelial-to-mesenchymal transition. Aging (Albany NY). 2020; 13(2):1947–61. https://doi.org/10.18632/aging.202158 PMID: 33323539

40. Yao T, Hu W, Chen J, Shen L, Yu Y, Tang Z, et al. Collagen XV mediated the epithelial-mesenchymal transition to inhibit hepatocellular carcinoma metastasis. J Gastrointest Oncol. 2022; 13(5):2472–84. https://doi.org/10.21037/jgo-22-299 PMID: 36388672

41. Thompson PW, Randi AM, Ridley AJ. Intercellular adhesion molecule (ICAM)-1, but not ICAM-2, acti-vates RhoA and stimulates c-fos and rhoA transcription in endothelial cells. J Immunol. 2002; 169 (2):1007–13. https://doi.org/10.4049/jimmunol.169.2.1007 PMID: 12097408

42. Puetz S, Lubomirov LT, Pfitzer G. Regulation of smooth muscle contraction by small GTPases. Physiol-ogy (Bethesda). 2009; 24:342–56. https://doi.org/10.1152/physiol.00023.2009 PMID: 19996365

43. van der Loop FT, Gabbiani G, Kohnen G, Ramaekers FC, van Eys GJ. Differentiation of smooth muscle cells in human blood vessels as defined by smoothelin, a novel marker for the contractile phenotype. Arterioscler Thromb Vasc Biol. 1997; 17(4):665–71. https://doi.org/10.1161/01.atv.17.4.665 PMID: 9108778

44. Ko YS, Yeh HI, Haw M, Dupont E, Kaba R, Plenz G, et al. Differential expression of connexin43 and desmin defines two subpopulations of medial smooth muscle cells in the human internal mammary artery. Arterioscler Thromb Vasc Biol. 1999; 19(7):1669–80. https://doi.org/10.1161/01.atv.19.7.1669 PMID: 10397684

45. Jin L. The actin associated protein palladin in smooth muscle and in the development of diseases of the cardiovasculature and in cancer. J Muscle Res Cell Motil. 2011; 32(1):7–17. https://doi.org/10.1007/s10974-011-9246-9 PMID: 21455759

46. Kai F, Fawcett JP, Duncan R. Synaptopodin-2 induces assembly of peripheral actin bundles and immature focal adhesions to promote lamellipodia formation and prostate cancer cell migration. Oncotarget. 2015; 6(13):11162–74. https://doi.org/10.18632/oncotarget.3578 PMID: 25883213

47. Yeh HI, Lupu F, Dupont E, Severs NJ. Upregulation of connexin43 gap junctions between smooth muscle cells after balloon catheter injury in the rat carotid artery. Arterioscler Thromb Vasc Biol. 1997; 17 (11):3174–84. https://doi.org/10.1161/01.atv.17.11.3174 PMID: 9409308

48. Hedin U, Bottger BA, Forsberg E, Johansson S, Thyberg J. Diverse effects of fibronectin and laminin on phenotypic properties of cultured arterial smooth muscle cells. J Cell Biol. 1988; 107(1):307–19. https://doi.org/10.1083/jcb.107.1.307 PMID: 2455726

49. Mercurius KO, Morla AO. Inhibition of vascular smooth muscle cell growth by inhibition of fibronectin matrix assembly. Circ Res. 1998; 82(5):548–56. https://doi.org/10.1161/01.res.82.5.548 PMID: 9529159

50. Asare-Amankwah Y, Riches-Suman K. The complex role of RhoA in regulating vascular smooth muscle cell phenotype in Type 2 diabetes. Vessel Plus. 2022; 6(64).

51. Rahuel C, Filipe A, Ritie L, El Nemer W, Patey-Mariaud N, Eladari D, et al. Genetic inactivation of the laminin alpha5 chain receptor Lu/BCAM leads to kidney and intestinal abnormalities in the mouse. Am J Physiol Renal Physiol. 2008; 294(2):F393–406. https://doi.org/10.1152/ajprenal.00315.2007 PMID: 18032551

52. Thyberg J, Blomgren K, Roy J, Tran PK, Hedin U. Phenotypic modulation of smooth muscle cells after arterial injury is associated with changes in the distribution of laminin and fibronectin. J Histochem Cytochem. 1997; 45(6):837–46. https://doi.org/10.1177/002215549704500608 PMID: 9199669

53. Mead TJ, Du Y, Nelson CM, Gueye NA, Drazba J, Dancevic CM, et al. ADAMTS9-Regulated Pericellular Matrix Dynamics Governs Focal Adhesion-Dependent Smooth Muscle Differentiation. Cell Rep. 2018; 23(2):485–98. https://doi.org/10.1016/j.celrep.2018.03.034 PMID: 29642006

54. Hadjiargyrou M. Mustn1: A Developmentally Regulated Pan-Musculoskeletal Cell Marker and Regulatory Gene. Int J Mol Sci. 2018; 19(1). https://doi.org/10.3390/ijms19010206 PMID: 29329193

55. Tello D, Balsa E, Acosta-Iborra B, Fuertes-Yebra E, Elorza A, Ordonez A, et al. Induction of the mitochondrial NDUFA4L2 protein by HIF-1alpha decreases oxygen consumption by inhibiting Complex I activity. Cell Metab. 2011; 14(6):768–79.

56. Pan P, Fu H, Zhang L, Huang H, Luo F, Wu W, et al. Angiotensin II upregulates the expression of placental growth factor in human vascular endothelial cells and smooth muscle cells. BMC Cell Biol. 2010; 11:36. https://doi.org/10.1186/1471-2121-11-36 PMID: 20500895

57. Shaw JH, Xiang L, Shah A, Yin W, Lloyd PG. Placenta growth factor expression is regulated by hydrogen peroxide in vascular smooth muscle cells. Am J Physiol Cell Physiol. 2011; 300(2):C349–55. https://doi.org/10.1152/ajpcell.00374.2010 PMID: 21123739

58. Xiang L, Varshney R, Rashdan NA, Shaw JH, Lloyd PG. Placenta growth factor and vascular endothelial growth factor a have differential, cell-type specific patterns of expression in vascular cells. Microcirculation. 2014; 21(5):368–79. https://doi.org/10.1111/micc.12113 PMID: 24410720

59. Newell LF, Holtan SG. Placental growth factor: What hematologists need to know. Blood Rev. 2017; 31 (1):57–62. https://doi.org/10.1016/j.blre.2016.08.004 PMID: 27608972

60. Newell LF, Holtan SG, Yates JE, Pereira L, Tyner JW, Burd I, et al. PlGF enhances TLR-dependent inflammatory responses in human mononuclear phagocytes. Am J Reprod Immunol. 2017; 78(4). https://doi.org/10.1111/aji.12709 PMID: 28635072

61. Yamazaki T, Mukouyama YS. Tissue Specific Origin, Development, and Pathological Perspectives of Pericytes. Front Cardiovasc Med. 2018; 5:78. https://doi.org/10.3389/fcvm.2018.00078 PMID: 29998128

62. Schubert K, Polte T, Bonisch U, Schader S, Holtappels R, Hildebrandt G, et al. Thy-1 (CD90) regulates the extravasation of leukocytes during inflammation. Eur J Immunol. 2011; 41(3):645–56. https://doi.org/10.1002/eji.201041117 PMID: 21264853

63. Giarratana N, Conti F, La Rovere R, Gijsbers R, Carai P, Duelen R, et al. MICAL2 is essential for myogenic lineage commitment. Cell Death Dis. 2020; 11(8):654. https://doi.org/10.1038/s41419-020-02886-z PMID: 32811811

64. Ferrari N, Ranftl R, Chicherova I, Slaven ND, Moeendarbary E, Farrugia AJ, et al. Dickkopf-3 links HSF1 and YAP/TAZ signalling to control aggressive behaviours in cancer-associated fibroblasts. Nat Commun. 2019; 10(1):130. https://doi.org/10.1038/s41467-018-07987-0 PMID: 30631061

65. Badri KR, Yue M, Carretero OA, Aramgam SL, Cao J, Sharkady S, et al. Blood pressure homeostasis is maintained by a P311-TGF-beta axis. J Clin Invest. 2013; 123(10):4502–12.

66. Santulli G. Angiopoietin-like proteins: a comprehensive look. Front Endocrinol (Lausanne). 2014; 5:4. https://doi.org/10.3389/fendo.2014.00004 PMID: 24478758

67. Dhanabal M, LaRochelle WJ, Jeffers M, Herrmann J, Rastelli L, McDonald WF, et al. Angioarrestin: an antiangiogenic protein with tumor-inhibiting properties. Cancer Res. 2002; 62(13):3834–41. PMID: 12097297

68. Xu Y, Liu YJ, Yu Q. Angiopoietin-3 inhibits pulmonary metastasis by inhibiting tumor angiogenesis. Cancer Res. 2004; 64(17):6119–26. https://doi.org/10.1158/0008-5472.CAN-04-1054 PMID: 15342395

69. Yang H, Liu J, Chen X, Li G. Angptl2 gene knockdown is critical for abolishing angiotensin II-induced vascular smooth muscle cell proliferation and migration. Biochem Cell Biol. 2022; 100(1):59–67. https://doi.org/10.1139/bcb-2021-0191 PMID: 34860608

70. Duan C, Clemmons DR. Differential expression and biological effects of insulin-like growth factor-binding protein-4 and -5 in vascular smooth muscle cells. J Biol Chem. 1998; 273(27):16836–42. https://doi.org/10.1074/jbc.273.27.16836 PMID: 9642243

71. Zheng Q, Xu X, Yang F, Gan H, Zhao Y, Wan X, et al. Single cell transcriptome analysis of decidua macrophages in normal and recurrent spontaneous abortion patients. bioRxiv. 2021.

72. Domanska D, Majid U, Karlsen VT, Merok MA, Beitnes AR, Yaqub S, et al. Single-cell transcriptomic analysis of human colonic macrophages reveals niche-specific subsets. J Exp Med. 2022; 219(3). https://doi.org/10.1084/jem.20211846 PMID: 35139155

73. Samaniego R, Dominguez-Soto A, Ratnam M, Matsuyama T, Sanchez-Mateos P, Corbi AL, et al. Folate Receptor beta (FRbeta) Expression in Tissue-Resident and Tumor-Associated Macrophages Associates with and Depends on the Expression of PU.1. Cells. 2020; 9(6).

74. Bohlson SS, O'Conner SD, Hulsebus HJ, Ho MM, Fraser DA. Complement, c1q, and c1q-related molecules regulate macrophage polarization. Front Immunol. 2014; 5:402. https://doi.org/10.3389/fimmu.2014.00402 PMID: 25191325

75. Li J, Diao B, Guo S, Huang X, Yang C, Feng Z, et al. VSIG4 inhibits proinflammatory macrophage activation by reprogramming mitochondrial pyruvate metabolism. Nat Commun. 2017; 8(1):1322. https://doi.org/10.1038/s41467-017-01327-4 PMID: 29109438

76. Samaniego R, Palacios BS, Domiguez-Soto A, Vidal C, Salas A, Matsuyama T, et al. Macrophage uptake and accumulation of folates are polarization-dependent in vitro and in vivo and are regulated by activin A. J Leukoc Biol. 2014; 95(5):797–808. https://doi.org/10.1189/jlb.0613345 PMID: 24399840

77. Puhlmann M, Weinreich DM, Farma JM, Carroll NM, Turner EM, Alexander HR Jr. Interleukin-1beta induced vascular permeability is dependent on induction of endothelial tissue factor (TF) activity. J Transl Med. 2005; 3:37. https://doi.org/10.1186/1479-5876-3-37 PMID: 16197553

78. O'Carroll SJ, Kho DT, Wiltshire R, Nelson V, Rotimi O, Johnson R, et al. Pro-inflammatory TNFalpha and IL-1beta differentially regulate the inflammatory phenotype of brain microvascular endothelial cells. J Neuroinflammation. 2015; 12:131.

79. Mackay F, Loetscher H, Stueber D, Gehr G, Lesslauer W. Tumor necrosis factor alpha (TNF-alpha)-induced cell adhesion to human endothelial cells is under dominant control of one TNF receptor type, TNF-R55. J Exp Med. 1993; 177(5):1277–86. https://doi.org/10.1084/jem.177.5.1277 PMID: 8386742

80. Moura R, Tjwa M, Vandervoort P, Cludts K, Hoylaerts MF. Thrombospondin-1 activates medial smooth muscle cells and triggers neointima formation upon mouse carotid artery ligation. Arterioscler Thromb Vasc Biol. 2007; 27(10):2163–9. https://doi.org/10.1161/ATVBAHA.107.151282 PMID: 17761938

81. Iruela-Arispe ML, Lombardo M, Krutzsch HC, Lawler J, Roberts DD. Inhibition of angiogenesis by thrombospondin-1 is mediated by 2 independent regions within the type 1 repeats. Circulation. 1999; 100(13):1423–31. https://doi.org/10.1161/01.cir.100.13.1423 PMID: 10500044

82. Taylor DS, Cheng X, Pawlowski JE, Wallace AR, Ferrer P, Molloy CJ. Epiregulin is a potent vascular smooth muscle cell-derived mitogen induced by angiotensin II, endothelin-1, and thrombin. Proc Natl Acad Sci U S A. 1999; 96(4):1633–8. https://doi.org/10.1073/pnas.96.4.1633 PMID: 9990076

83. Nibbs RJ, Graham GJ. Immune regulation by atypical chemokine receptors. Nat Rev Immunol. 2013; 13(11):815–29. https://doi.org/10.1038/nri3544 PMID: 24319779

84. Szentivanyi M Jr., Berczi V, Huttl T, Reneman RS, Monos E. Venous myogenic tone and its regulation through K+ channels depends on chronic intravascular pressure. Circ Res. 1997; 81(6):988–95. https://doi.org/10.1161/01.res.81.6.988 PMID: 9400379

85. Hakibilen C, Delort F, Daher MT, Joanne P, Cabet E, Cardoso O, et al. Desmin Modulates Muscle Cell Adhesion and Migration. Front Cell Dev Biol. 2022; 10:783724. https://doi.org/10.3389/fcell.2022.783724 PMID: 35350386

86. Javed E, Thangavel C, Frara N, Singh J, Mohanty I, Hypolite J, et al. Increased expression of desmin and vimentin reduces bladder smooth muscle contractility via JNK2. FASEB J. 2020; 34(2):2126–46. https://doi.org/10.1096/fj.201901301R PMID: 31909533

87. Sartore S, Chiavegato A, Faggin E, Franch R, Puato M, Ausoni S, et al. Contribution of adventitial fibro-blasts to neointima formation and vascular remodeling: from innocent bystander to active participant. Circ Res. 2001; 89(12):1111–21. https://doi.org/10.1161/hh2401.100844 PMID: 11739275

88. Newman AC, Nakatsu MN, Chou W, Gershon PD, Hughes CC. The requirement for fibroblasts in angio-genesis: fibroblast-derived matrix proteins are essential for endothelial cell lumen formation. Mol Biol Cell. 2011; 22(20):3791–800. https://doi.org/10.1091/mbc.E11-05-0393 PMID: 21865599

89. Hao Y, Hao S, Andersen-Nissen E, Mauck WM 3rd, Zheng S, Butler A, et al. Integrated analysis of mul-timodal single-cell data. Cell. 2021; 184(13):3573–87.e29. https://doi.org/10.1016/j.cell.2021.04.048 PMID: 34062119

90. McGinnis CS, Murrow LM, Gartner ZJ. DoubletFinder: Doublet Detection in Single-Cell RNA Sequenc-ing Data Using Artificial Nearest Neighbors. Cell Syst. 2019; 8(4):329–37.e4. https://doi.org/10.1016/j.cels.2019.03.003 PMID: 30954475

91. Young MD, Behjati S. SoupX removes ambient RNA contamination from droplet-based single-cell RNA sequencing data. Gigascience. 2020; 9(12). https://doi.org/10.1093/gigascience/giaa151 PMID: 33367645

92. Korsunsky I, Millard N, Fan J, Slowikowski K, Zhang F, Wei K, et al. Fast, sensitive and accurate inte-gration of single-cell data with Harmony. Nat Methods. 2019; 16(12):1289–96. https://doi.org/10.1038/s41592-019-0619-0 PMID: 31740819

93. Cao J, Spielmann M, Qiu X, Huang X, Ibrahim DM, Hill AJ, et al. The single-cell transcriptional land-scape of mammalian organogenesis. Nature. 2019; 566(7745):496–502. https://doi.org/10.1038/s41586-019-0969-x PMID: 30787437

94. Yu G, Wang LG, Han Y, He QY. clusterProfiler: an R package for comparing biological themes among gene clusters. OMICS. 2012; 16(5):284–7. https://doi.org/10.1089/omi.2011.0118 PMID: 22455463

95. Jin S, Guerrero-Juarez CF, Zhang L, Chang I, Ramos R, Kuan CH, et al. Inference and analysis of cell-cell communication using CellChat. Nat Commun. 2021; 12(1):1088. https://doi.org/10.1038/s41467-021-21246-9 PMID: 33597522